Final Technical Report
Project A-2668

ICE/FROST DETECTION USING MILLIMETER WAVE RADIOMETRY

J. A. Gagliano, J. M. Newton, A. R. Davis,
and M. L. Foster

Final Report for Period 28 May 1980 - 31 August 1981

31 August 1981

Prepared For

NASA George C. Marshall Space Flight Center
MSFC, Alabama 35812

NASA Contract NAS8-33800

Prepared By

Georgia Institute of Technology
Engineering Experiment Station
Atlanta, Georgia 30332

1 Report No	2 Government Accession No	3 Recipient's Catalog No
A-2668		N81 321 76

4 Title and Subtitle	5 Report Date
Ice/Frost Detection Using Milimeter Wave Radiometry	August 31, 1981
	6 Performing Organization Code
7 Author(s)	8 Performing Organization Report No
J.A. Gagliano and others	
9 Performing Organization Name and Address	10 Work Unit No
Georgia Institute of Technology Engineering Experiment Station Atlanta, Georgia 30332	11 Contract or Grant No NAS8-33800
	13 Type of Report and Period Covered Final Technical Report 5/28/80 to 8/31/81
12 Sponsoring Agency Name and Address	14 Sponsoring Agency Code
NASA Marshall Space Flight Center Huntsville, Alabama 35812 Project Manager, E.H. Gleason	EC 33

15 Supplementary Notes

16 Abstract

A series of ice detection tests were performed on the shuttle external tank (ET) and on ET target samples using the Georgia Tech 35/95GHz instrumentation radiometer. The ET target sample tests were performed at Georgia Tech using a test enclosure containing ET Spray-On-Foam-Insulation (SOFI) samples. Ice was formed using liquid nitrogen and water spray inside the Georgia Tech designed test enclosure. The shuttle ET tests were performed at NASA's National Space Technology Laboratory (NSTL) during cryogenic fueling operations prior to the shuttle orbiter engine firing tests. Ice was formed with freon and water over a one meter square section of the ET LOX tank. Data analysis was performed on the ice signatures, collected by the radiometer, using Georgia Tech computing facilities. Data analysis techniques developed during this program include: ice signature images of scanned ET target; pixel temperature contour plots, time correlation of target data with ice present versus no ice formation; and ice signature radiometric temperature statistical data, i.e. mean, variance, and standard deviation.

17 Key Words (Selected by Author(s))	18 Distribution Statement
95GHz, Multichannel scanning radiometer, Data Collection Processor, Ice signature analysis	

19 Security Classif (of this report)	20 Security Classif (of this page)	21 No of Pages	22 Price*
Unclassified	Unclassified	55	

*For sale by the National Technical Information Service, Springfield, Virginia 22151

Table of Contents

List of Figures

List of Tables

1.0 Introduction

In accordance with Contract No. NAS8-33800 for NASA/MSFC, Georgia Tech has investigated the use of an advanced instrumentation radiometer operating at 35/95 GHz to detect the presence of ice on the space shuttle external tank (ET). Other methods used in the past to detect ice formation have included infrared (IR) sensors, TV camera display, visual observations, and thermocouples. The need for remote operation a distance from the launch site eliminates visual observation just prior to launch. A TV display has not demonstrated accuracy in verifying the presence of ice from a remote location several hundred feet from the external tank. Thermocouples measure the actual temperature of the ET surface so that frost, ice and cold, clear areas would not be distinguishable. In addition, a large number of thermocouples would be needed to cover the entire ET target for ice detection. Finally, sensing devices operating in the millimeter wave spectrum can penetrate rain, fog, or dust with more effectiveness than IR sensors due to the lower propagation loss at millimeter wave lengths.

Table 1 is a summary of activities performed by Georgia_Tech during the period of this contract. These activities were performed with the purpose of demonstrating that millimeter wave radiometry techniques could be used to detect ice formation on target samples at Georgia Tech and on the ET following cryogenic loading operations at NASA's shuttle test facility in Mississippi.

Samples of the shuttle external tank (ET) Spray-On-Foam-Insulation (SOFI) target were utilized during the measurements performed at Georgia Tech. This activity formed the basis of the measurement task performed by Georgia Tech to evaluate the ice/frost signature under varying conditions for weather, target viewing angle and distance. Table 2 summarizes the major activities associated with Phase 1a measurements.

Upon evaluation by NASA of the ice signature data collected at Georgia Tech, a request was made to perform additional measurements at the NASA National Space Technology Laboratory (NSTL) near Bay St. Louis,

Table 1

Ice Detection Program Summary

Phase	Activity	Status
1a	Performed ice/frost detection measurements on external tank (ET) samples under varying environment conditions using the existing Georgia Tech millimeter wave radiometer operating at 95 GHz.	Contract No. NAS8-33800
1b	Used existing Georgia Tech instrumentation radiometer to perform additional ice/ frost measurements on shuttle ET during actual cryogenic loading procedures at National Space Technology Laboratory (NSTL) in Mississippi.	NAS8-33800 Contract Mod. #2
1c	Modified existing Georgia Tech 35/95 GHz radiometer for improved spatial resolution with the addition of a 4-foot dish and further analysis of ice signature data gathered at NSTL.	NAS8-33800 Contract Mods #3 & #4

Table 2

Ice Detection Activities at Georgia Tech (Phase 1a)

Activity	Comment
Scan reference target concurrent with ET target	Compensate for variation in sky background during radiometric scan
Scan dry spray-on-foam-insulation (SOFI) ET sample	Average pixel difference of 3°K between ET and reference targets
Scan ice covered SOFI ET Sample	Average pixel difference of 49°K between ET and reference targets
Printout pixel temperature contour plots of ET and reference targets	Multiple pixel temperature data per target
Display radiometric imaged scan for each data run	Imaged scan corresponds to pixel temperature printout
Vary ET sample target viewing angle for different data runs	Ice detected on target for all viewing angle runs

Mississippi where the shuttle external tank was undergoing cryogenic loading procedures. This task offered a good opportunity for Georgia Tech to obtain ice signature data on the ET during cryogenic loading operations in order to detect ice formation. For the measurements at Georgia Tech, a significant effort was put into the formation of ice on the target using a Georgia Tech designed test enclosure. The measurements at NSTL allowed for complete dedication to the task of detecting ice on the ET and for processing the data in real time using the Georgia Tech Data Collection Processor (DCP). Table 3 summarizes the activities performed at NSTL.

Following the measurements at NSTL, NASA requested that Georgia Tech improve the spatial resolution of the radiometer in preparation for proposed future tests on the shuttle ET at Kennedy Space Center (KSC). For this task Georgia Tech replaced the 20 inch lens antenna with a 4 foot dish which reduced the beam spot diameter to approximately 1.7 feet at a distance of 450 feet from radiometer to target. Antenna pattern measurements, performed at Georgia Tech, yielded a 3 dB beamwidth of 0.22° at 95 GHz.

A continuing task throughout the ice detection program was the data analysis effort performed by Georgia Tech on the data collected during the measurements. The analysis techniques were performed using the radiometer's DCP, Georgia Tech's Eclipse computer system, and the on-campus Cyber computer facility. Data processing techniques included. near real-time imaging of the scanned target; hard copy printouts of data run header information and calibration data; pixel temperature contour plotting; ice signature radiometric temperature statistical data, i.e., mean, variance, and standard deviation; and time correlation of target data with and without ice formation.

The ice detection program performed by Georgia Tech has led to a viable means to detect the formation of ice on the ET surface using a millimeter wave scanning radiometer. It has been demonstrated that a dedicated sensor could be built and located near the space shuttle launch facility in the future. Figure 1 depicts the operational

Table 3

Shuttle ET Ice Detection Activities at NSTL (Phase 1b)
Performed in December 1980 and January 1981

Activity	Comment
Scan reference targets (2) concurrent with ET	Compensate for sky background variation using bare metal and SOFI reference targets
Integrate elevation tachnometer into instrumentation radiometer	Maintain constant scan speed for varying torque with elevation angle near 25 degrees
Eight hours of continuous radiometric scans of ET with scan repeated every 30 minutes	ET scanning continuous from pre-loading of cryogenic to post-firing of orbiter engines
Scan ET cut-out section of 1 meter square having reduced foam thickness	Ice was formed on cut-out region following loading and was detected by 95 GHz radiometer
Generate on-line radiometric images of scanned ET after tank is loaded	Average brightness temperature increase of about 20K observed on cut-out section with ice present

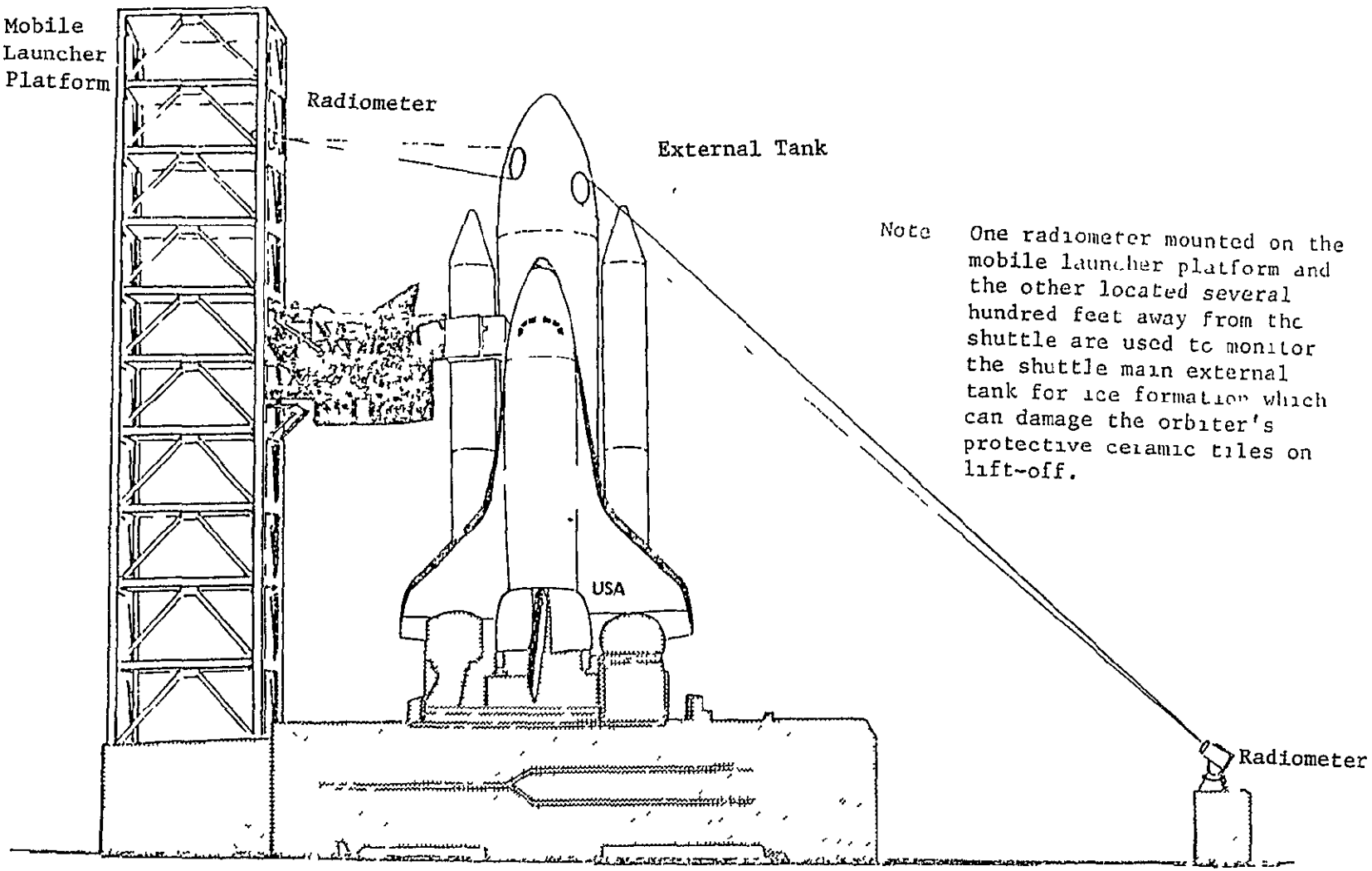

Figure 1. Shuttle Launch Facility Showing Ice Detection Radiometer Systems.

configuration of two millimeter wave sensors located at the shuttle launch facility which would provide ET surface monitoring from remote sites. The data analysis algorithms developed by Georgia Tech have demonstrated that on-line processing of ice signature could be performed prior to a shuttle launch operation. The results of the data processing could be used to aid in NASA's decision as to a go or no-go launch of the shuttle due to the accumulation of ice on the external tank.

2.0 Technical Discussion

2.1 Radiometric Measurement Techniques

The measurements at Georgia Tech and NSTL were performed using the 35/95 GHz instrumentation scanning radiometer developed by Georgia Tech. Figure 2 is a photograph of the Georgia Tech radiometer used for all ice detection measurements performed during this program. For the measurements performed at Georgia Tech the target scanned was an ET sample with SOFI. Figure 3 is a photograph of the target chamber designed by Georgia Tech for these measurements. An aluminum plate of 1/2 inch thickness located inside the chamber served as a liquid nitrogen reservoir for reducing the target temperature to below freezing. The target sample of dimensions 3 feet by 3 feet by 1/4 inch SOFI thickness was mounted to this aluminum plate. Horizontal pivot bearings on each side of the target chamber allowed for a variation in the target deflection angle over a nominal range of 30° to 60°.

The measurements at NSTL were performed on a shuttle external tank (ET) undergoing cryogenic loading prior to orbiter engine firing operations. Figure 4 is a view of the ET as seen from the radiometer located about 450 feet away. This is the general area from which the Georgia Tech 35/95 GHz radiometer scanned the ET during cryogenic loading operations. The spatial resolution (beam spot diameter on target) for the radiometer is a function of the sensor's antenna size, operating frequency, and distance from the target to the radiometer. Figure 5 depicts the geometry for the ice detection measurements using the ET as the target scanned. For these measurements, the 95 GHz radiometer had a 0.4° half power beamwidth (θ_B°) using a 20 inch diameter (D) lens. The beam spot diameter (d) on target at a range R from the radiometer is given by:

$$d = R\theta_B^\circ \frac{\pi}{180} .$$

The beam spot diameter varied with the radiometer to target range, R, according to the above equation. For the NSTL measurements at 95 GHz and a range of 450 feet, the beam spot diameter on target is given by:

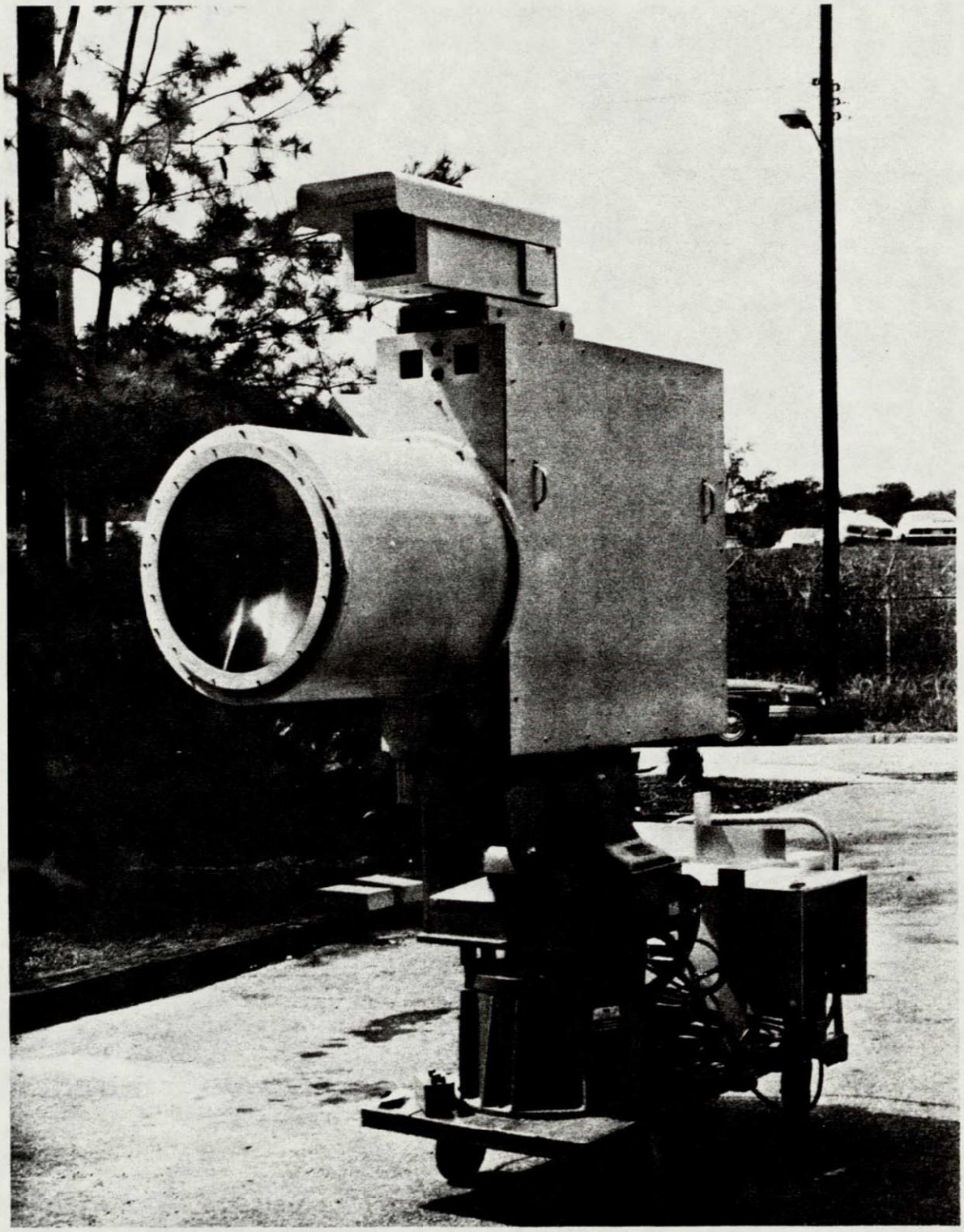

Figure 2. Radiometer Assembly - Front View.

ORIGINAL PAGE IS
OF POOR QUALITY

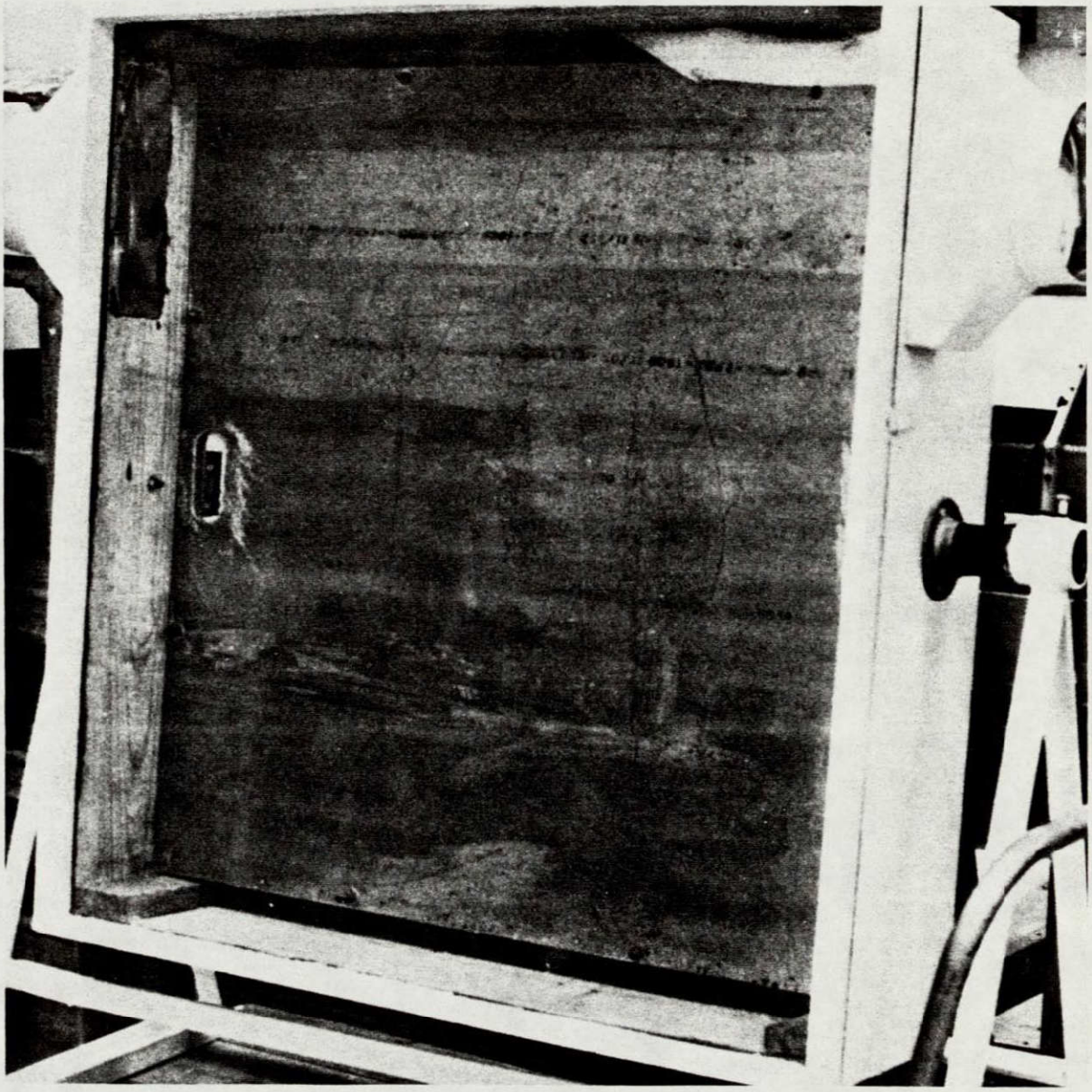

Figure 3. Ice/Frost Detector Test Enclosure for External Tank Target Samples.

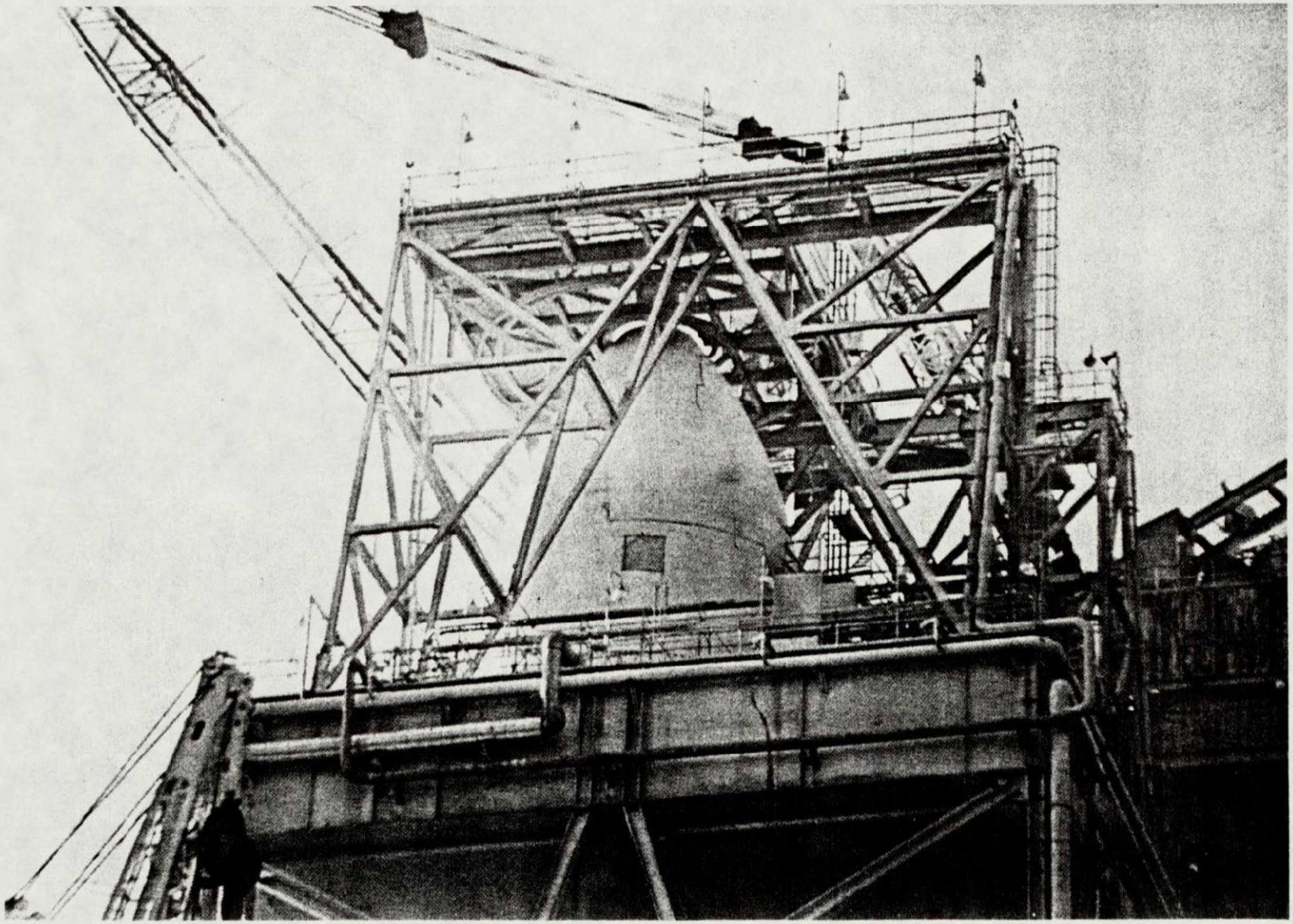

Figure 4. View of External Tank at NSTL Facility as Seen from Georgia Tech Radiometer.

$$d = (450)(0.4)\frac{\pi}{180}$$

$$= 3.14 \text{ feet.}$$

Since the ET diameter is approximately 28 feet, then the number of beam spots across the target was 28/3.14 = 8.9 beam spots per scan across the ET diameter.

2.2 Radiometer Hardware Description

Figure 6 is a detailed block diagram of the scanning millimeter wave radiometer used for performing ice/frost signature measurements. The radiometer and associated instrumentation consists of the following elements: internal hot/cold load calibration system, 35 GHz RF head (scene and sky viewing), 95 GHz RF head (scene and sky viewing), TV camera unit (scene truth), a rotary platform for the sensors, radiometer receiver (IF amplifiers, filters, square law detectors, synchonous detectors, and integrators), microcomputer based data acquisition system, and a reel-reel tape recorder. A pictorial diagram of the system is shown in Figure 7. The measurement radiometer provides precise scene resolution, low noise operation for good temperature resolution, adequate stabilization of electronics for good temperature resolution, and good absolute temperature measurement accuracy.

The radiometer performs dual frequency measurements by using the super chopper design implemented on other programs at Georgia Tech as shown in Figure 8. The 35 GHz/95 GHz feed horns receive the signal from the scene (target), sky view, or internal calibration loads as selected by the data acquisition system (DAS). The signal exits via the horizontally (H) and vertically (V) polarized output ports of the orthomode transducer. Each polarized signal is down-converted in a separate mixer to an IF of nominally 2.0 to 4.0 GHz. The local oscillator signal is injected into each mixer using a directional filter.

The IF is split off using a 4-way power divider into two bandpass filters and two termination loads. These bandpass filters provide passbands of 1 GHz and 2 GHz centered on 3 GHz. The two extra ports, which are terminated, are spare paths for future growth that could be used with different bandpass filters or be used for IF correlation of the H and V channels. Square law detectors follow each bandpass filter. The detected Dicke modulated signal in each channel goes to a phase

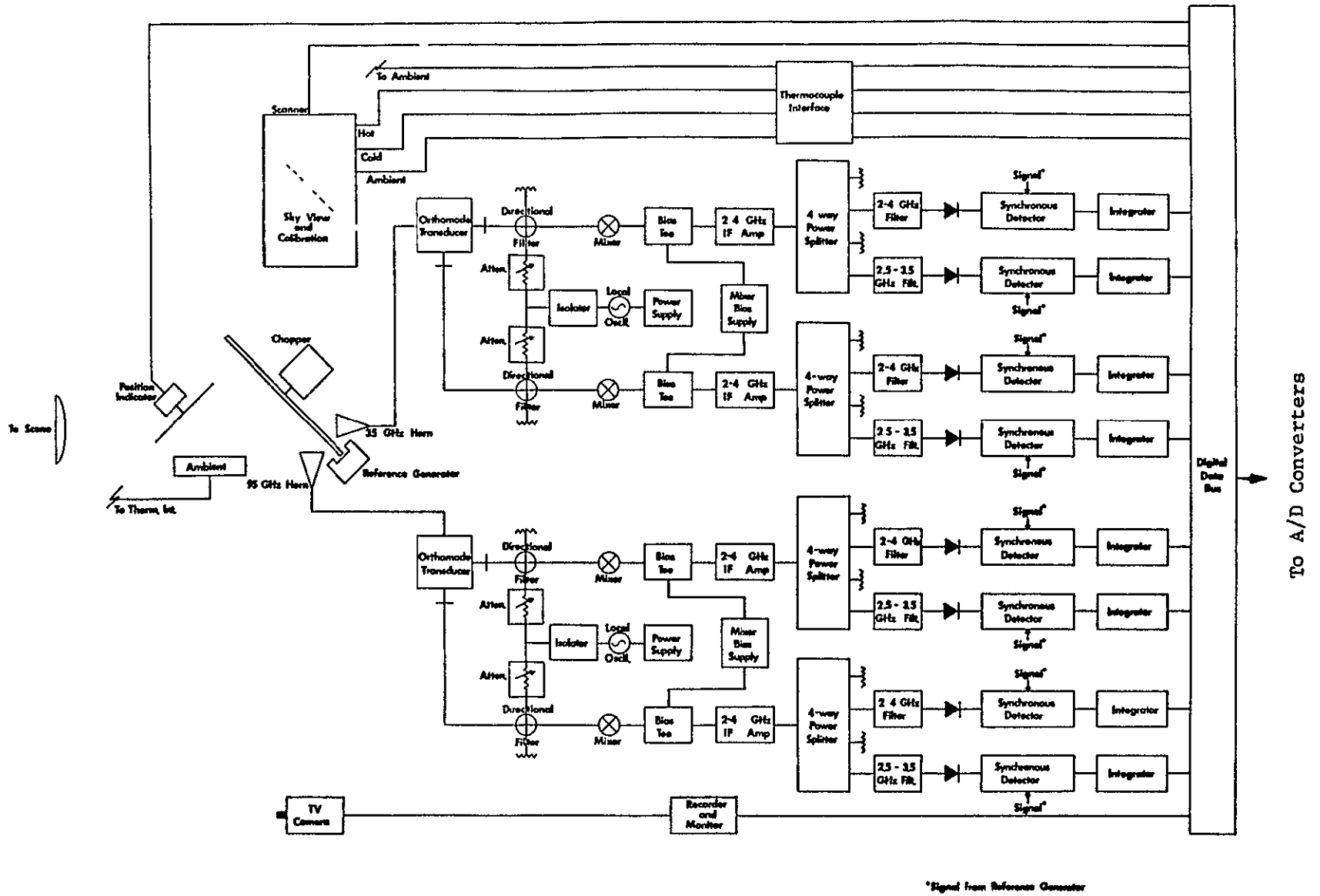

Figure 6. Block Diagram of Radiometer.

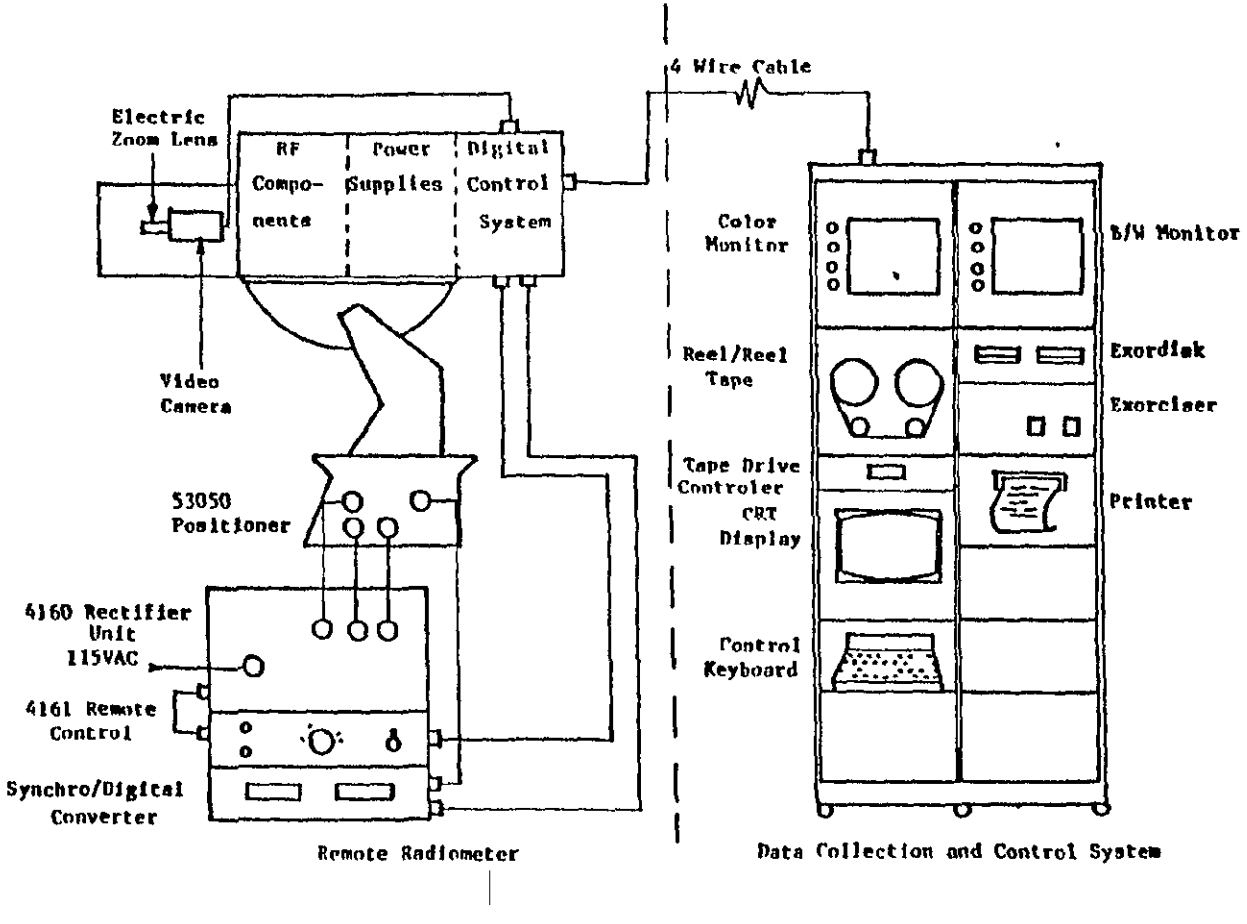

Figure 7. Millimeter-Wave Instrumentation Radiometer.

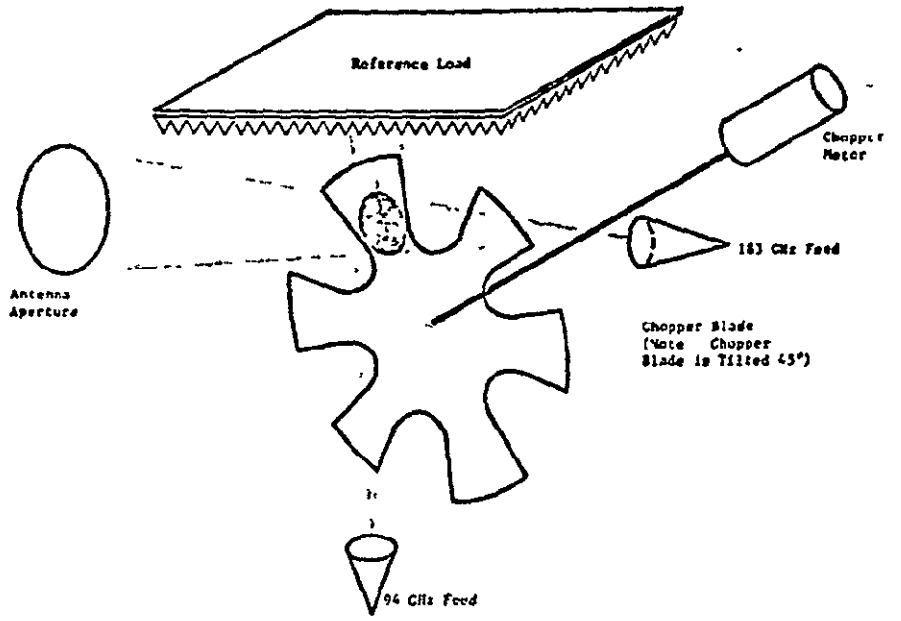

(a) Super-Chopper Concept - Shown Reflecting To Antenna At 94 GHz and Reflecting Into Reference Load at 183 GHz

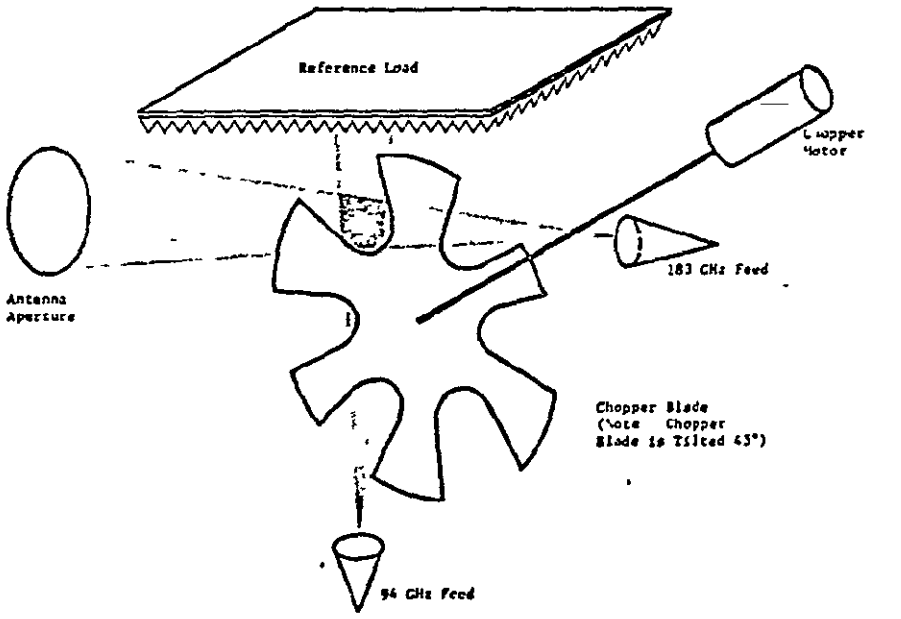

(b) Super-Chopper - Shown Transmitting To Reference Load at 94 GHz and Transmitting to Antenna at 183 GHz

Figure 8. 94/183 GHz Radiometer Super Chopper Concept.

sensitive detector (PSD) whose input is multiplied by the super chopper reference generator. The reference signal switches the detector output in synchronization with the antenna signal so that the PSD output voltage is directly proportional to the scene temperature. The integrator is a low-pass filter having an integration time chosen to yield an acceptable temperature resolution. All integrator outputs are routed to the data acquisition system.

2.2.1 RF system

The RF portion of the radiometer consists of a dual frequency, dual polarization receiver as shown in Figure 9. The two frequencies share a common radiating aperture as well as common calibration loads. This is accomplished by integrating two feeds using the super chopper. The feeds are corrugated conical horns and are mounted orthogonal to each other so that as the chopper rotates, the feeds look alternately at the Dicke load and the scene. Since the assembly is symmetrical, no depolarization takes place. Therefore, both E_ϕ and E_θ polarization components are equally received.

A 6 inch diameter Rexolite lens, having an f/D ratio of 1, is illuminated by the horns. This lens focuses energy from the horn to a spot 6 inches from the lens so that beam switching may be easily accomplished. The focused beam can be reflected by the small switching reflector into one of the calibration loads or can be allowed to pass unblocked. The unblocked beam illuminates the 20 inch radiating aperture.

The 20 inch lens is designed to correct the phase of the incoming RF signal so that it is focused at the correct target range. Adjustments of the focal distance is accomplished by moving the 20 inch lens along the lens/horn axis. Single frequency antenna patterns measured at the focal point, in the target plane, show the antenna to have a 0.4 degree 3 dB beamwidth at 95 GHz and sidelobes greater than 24 dB below the peak signal. The 35 GHz pattern exhibits the same sidelobe structure but has a 3 dB beamwidth of 1.3 degrees.

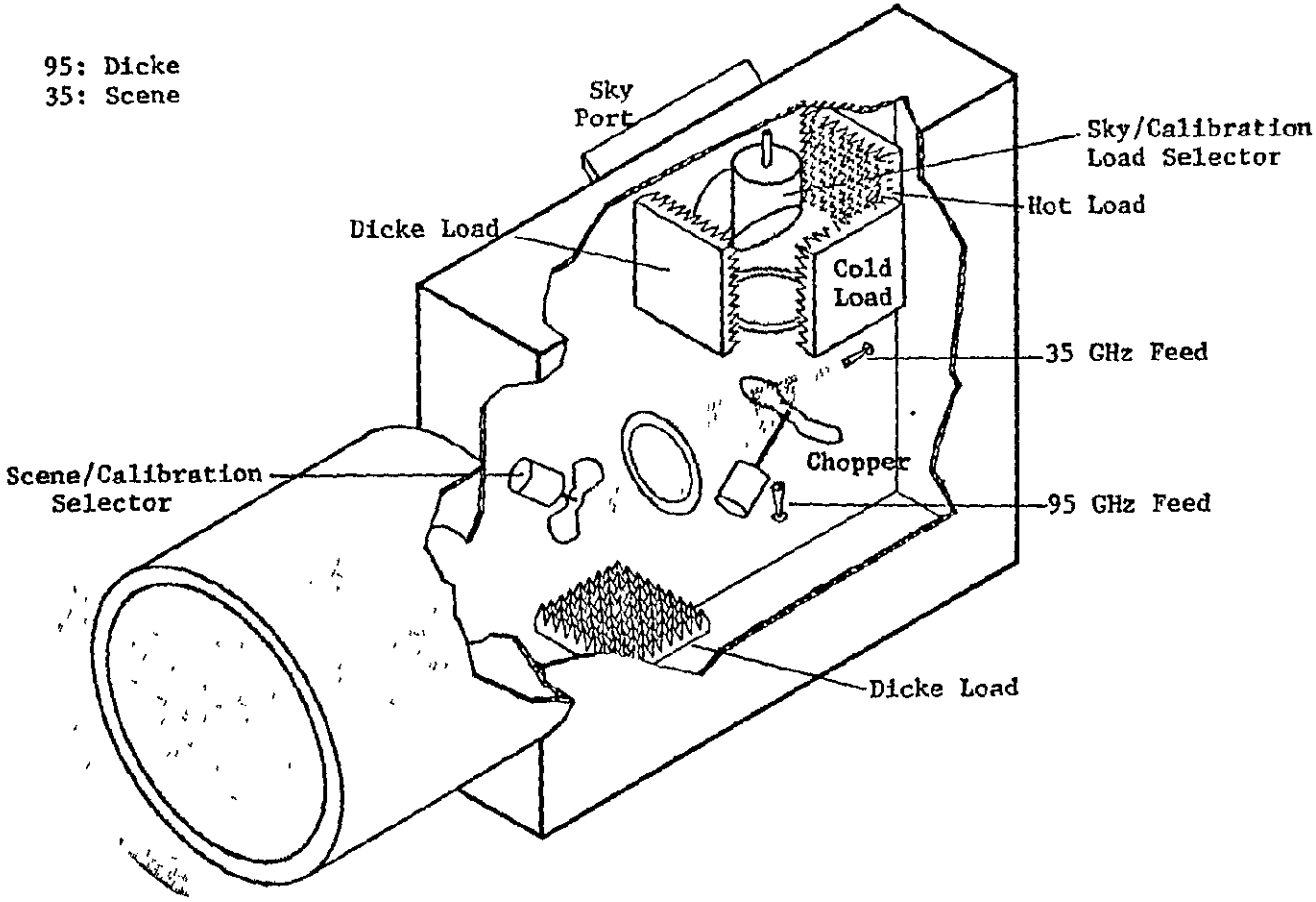

Figure 9 RF Portion of Radiometer.

Signals received by the corrugated conical horns are transmitted to a waveguide orthomode coupler where they are split into E_ϕ and E_θ polarization components. These signals are down-converted to the 2-4 GHz IF band. A coupling device other than the standard directional coupler is required so as to keep the losses in the mixer chain low, while providing low insertion loss for the local oscillator signal. The coupling device used in this radiometer is actually a directional filter (having a very small range of frequencies) such that transmission can occur at the LO frequency. Outside this frequency range the input signal bypasses the coupling structure resulting in negligible losses at the signal frequency.

One of the antenna feeds shown in Figure 9 views an ambient temperature load, used as the Dicke reference, while the other feed views either a scene with an unknown temperature (data mode) or a known temperature reference load (calibration mode). During data collection the lower port views the scene through the large lens while the upper port views the Dicke reference load. For calibration the lower port is reflected to view the second Dicke reference load. The upper port views the sky (via the sky reflector), the hot load, the cold load, and the upper Dicke reference load. Both the upper and lower reflectors are positioned by stepper motors under microcomputer control.

The calibration and reference loads consist of pyramids made with an absorbing material adequate for both polarizations. The pyramids are cut at the Brewster angle to minimize reflections. The hot load is temperature controlled with heating elements and the cold load is cooled with liquid nitrogen. The cold load temperature is monitored by thermistors routed thru a multiplexor to the computer. Thermistors are also used to measure the operating temperature of several major RF components including the large lens.

2.2.2 IF/Video System

The IF/Video portion of the radiometer consists of the IF amplifiers, filters, square law detectors, video amps, and phase sensitive detectors. The IF section is identical for each of the four frequency and polarization combinations. The IF signal is nominally 2.0 to 4.0 GHz. It is amplified by two IF amplifiers each of which provides approximately 35 dB of gain. The amplifier output is fed into a four-way power splitter. Two ports of the power splitter are terminated in matched loads providing spare paths for possible future growth. The other two ports feed bandpass filters with passbands of 1 GHz and 2 GHz centered on 3 GHz. The 1 GHz filter has 9 elements giving a very steep rolloff outside the passband. The 2 GHz filter has 2 elements giving a less steep rolloff characteristic. Each filter is followed by a Schottky diode square law detector.

The detected Dicke modulated signal goes to a video amplifier having a voltage gain of 2000. This signal is fed to the phase sensitive detector (PSD). The first stage of the PSD is a high Q bandpass filter centered on the Dicke chopping frequency. This signal is multiplied with the chopper reference signal giving a full wave rectified signal with a voltage directly proportional to the scene temperature. The signal is then integrated by a low-pass filter having an integration time of approximately 0.25 seconds. At this point the signal is a dc voltage directly proportional to the scene temperature. The integrator output is routed to the data acquisition system.

2.2.3 Radiometer Auxiliary Equipment

Radiometer auxiliary equipment includes the antenna positioner and associated controls, the television camera, and the turntable controls. A Scientific Atlanta 54050 antenna positioner was used to rotate the radiometer during the measurements at Georgia Tech and NSTL. The 54050 positioner is an elevation-over-azimuth unit that allows the measurement of true vertical and horizontal polarization.

The positioner is controlled by the microcomputer via a Georgia Tech built interface. The computer sends an axis selection, a direction selection, and a speed voltage to the interface which routes these signals to the positioner. Each axis of the positioner has two synchro position indicators (a 1:1 and a 36:1). The computer-positioner interface converts the synchro outputs to binary coded decimal angles and routes these signals to the computer. The angle readouts are to .01 degrees and the positioner is positioned to 0.10 (+ 0.09/-0.00) degree accuracy.

A television camera is used to provide a record of the scene imaged by the radiometer and also to set up the limits of scan patterns. The camera is initially aligned with the center of the field-of-view of the radiometer antenna. After the transmitter is centered in the field-of-view of the radiometer, the camera lens is adjusted to the same field-of-view. The image of the transmitting antenna is then brought into view of the camera by adjusting the camera mount alignment with respect to the radiometer. The camera mount provides a rigid support to maintain this initial alignment. The television camera's iris opening, focus, and zoom lens are controlled from the operator's console via the computer. The camera field-of-view can thus be matched to the radiometer field-of-view and the iris can be adjusted to cope with changing light conditions.

2.3 Radiometer Data Acquisition System

The radiometer data acquisition system consists of two major units under the control of separate microprocessors. The first unit, known as the Radiometer Interface Processor (RIP), is located within the radiometer enclosure and provides the link between the analog radiometer hardware and the other unit. The second unit, known as the Data Collection Processor (DCP), is located in a dual rack assembly which can be separated up to 300 feet from the radiometer. The DCP contains the receiver for the RIP output and the transmitter for commands. Radiometric and calibration data from sensors in the radiometer are digitized by the RIP and passed to the DCP which records the data on magnetic tape. Control signals from the DCP are routed to the radiometer by the RIP so as to operate the two-axis positioner, control the chopper and stepper motors, and to calibrate the radiometer. Figure 10 is a photograph of the DCP used during the measurements.

The data acquisition system insures that target data is recorded reliably and accurately in a form that will simplify analysis on a computer. The software and hardware of the radiometer data acquisition system allowed unattended operation during the actual measurements and insured the quality and integrity of the data. Among the functions automated by the data acquisition system were the scanning of the external tank scene raster by the radiometer. An algorithm was formulated to compute all the locations where sampling would occur from three sets of input coordinates representing the size and centroid depression angle of the desired raster frame.

2.3.1 Data Acquisition Components

The RIP performs three major functions: 1) convert analog outputs from the eight radiometer channels and 12 thermistors into digital data, 2) accept commands from the DCP to control the movement of the calibration reflectors, antenna positioner, and zoom lens, and 3) send digital data and status data to the DCP for recording.

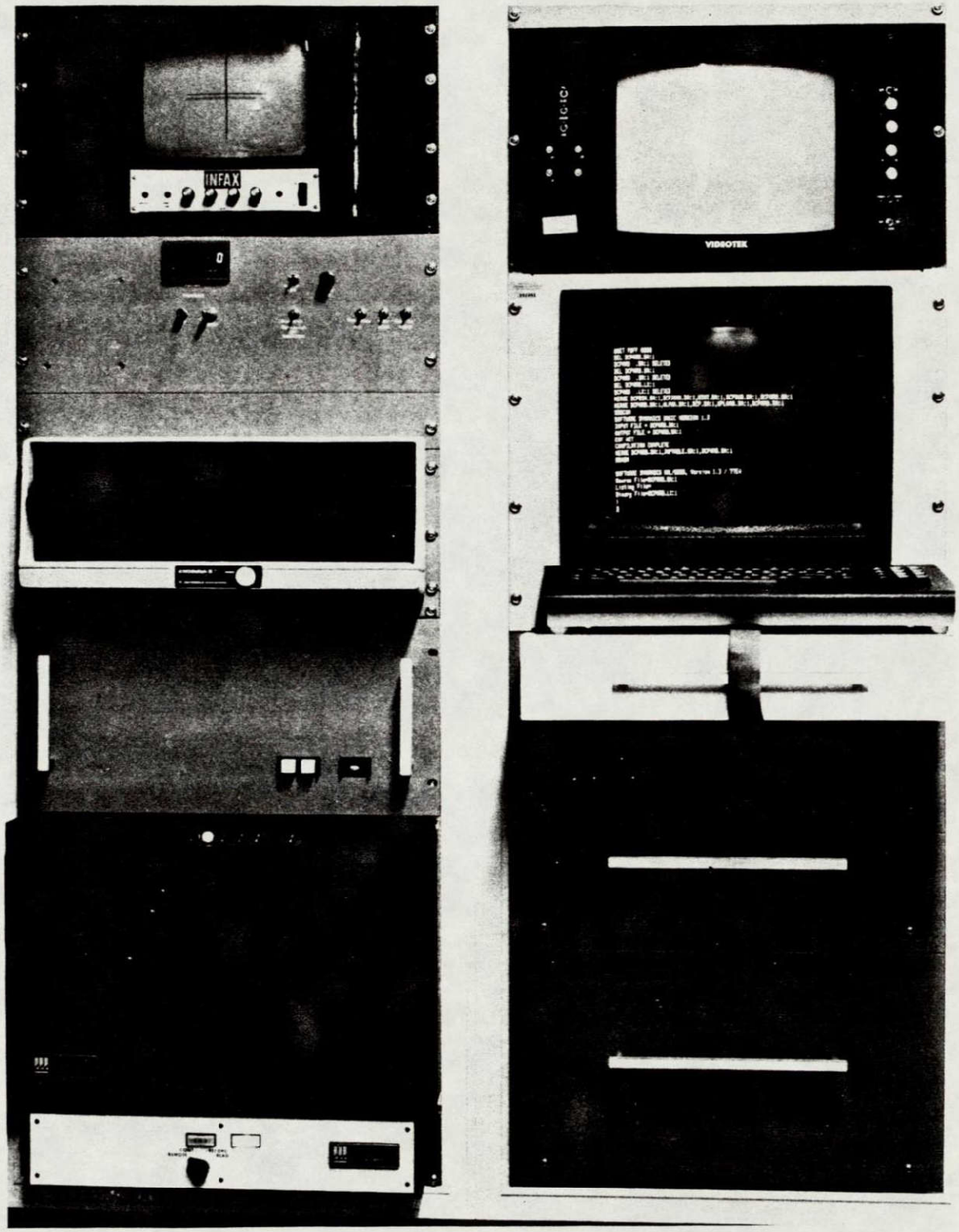

Figure 10. Photograph of Georgia Tech Radiometer's Data Collection Processor (DCP).

the data acquisition system. This device allowed permanent storage of the operating system software and also was used for temporary storage of radiometric data prior to being formatted for writing on magnetic tape.

The operator header information, the video image, and the ice signature and calibration data were recorded on magnetic tape. All data tapes produced on the 35/95 GHz instrumentation radiometer data collection processor conform to the ANSII standard for reel-to-reel 1-/2" magnetic tapes. The particular equipment utilized to record these tapes is a Digi-Data Corp. Model 1639 transport and a Digi-Data Model LP-PE-9H2 dual buffer/formatter. Data was recorded in nine track, 1600 bits per inch, phase encoded IBM compatible format on a 8-1/2" reel. All tape records are a fixed length of 1024 bytes. Approximately 12 megabytes of storage capacity are available per one 8-1/2" reel.

Graphical representations of the ET surface were displayed on a video monitor driver by a graphics generator. The format of the display was controlled by appropriate software in the DCP microcomputer. A resolution of 256 x 256 points with a 16 level gray or color scale was provided. A black and white image of the target was digitized and stored to allow correlation between measured ET target temperatures and actual ET target geometry. A CRT terminal was used to provide an interface between the operator and the data acquisition system. The operation of the radiometer was controlled by commands entered via the CRT terminal keyboard and all messages from the system were displayed on the terminal. A time of day clock with battery backup power provided the current date and time to the nearest second for the microcomputer. This time information was needed for scan sequencing timing. The clock was set via commands from the CRT terminal.

2.3.2 RIP Software Description

The radiometer interface processor (RIP) software is a BASIC-language program which implements commands from the data collection processor (DCP) and sends data back to the DCP. The software consists of five main sections - initialization routine, the main program, command execution subroutines, input-output routines, and

interrupt service routines. The initialization routine is executed once at the beginning of the program. It initializes all variables and memory locations to the proper values. The main program receives commands from the DCP and decodes them. It then transfers control to the correct subroutine for execution of that command. After the command has been implemented, the command is echoed to the DCP and the program is ready to go on to the next command.

The command execution subroutines are called by the main program or other subroutines and implement the various functions of the radiometer. These routines control the reflector positioning motors, the zoom lens functions, the antenna positioner, and the analog to digital converter. There are also subroutines to execute a scan and to perform a calibration. After implementing the command, program control is returned to the main program or the calling subroutine.

The input-output routines control data transmission and reception through a two-way serial link between the RIP and the DCP. There are two types of routines in this section. The primitive routines control data on a single character level. The other routines handle formatted data. The last section of the software contains the interrupt service routines. There are two types of interrupts, both of which are routed through the main program. An interrupt from the DCP will cause the transmission of the output data buffer when this interrupt is enabled. An interrupt from the antenna positioner results in an update of the appropriate angle. During data collection this interrupt also causes a check for a valid data point and collection of the radiometer channel voltages if the angle is valid.

2.3.3 DCP Software Description

The DCP software is a combination of BASIC and assembly language programs. It can be separated into two major areas, 1) implement commands from the operator to execute a data scan and record the gathered data and 2) analyze the recorded data to verify proper operation of the radiometer.

The initialization routine is executed at the beginning of the program. It initializes all variables for the DCP software and accepts

commands from the operator. The adjust positioner and camera routine instructs the operator to position the radiometer to the center of the target and set the field of view and focus of the B/W camera through panel switches. The appropriate commands are relayed to the RIP. The actual position (angles) of the radiometer is saved for reference and a digitized B/W image is recorded. The operator is instructed to move the positioner to the top center, then to the left center of the target area. Using the operator-generated target parameters, the appropriate pattern points are calculated to provide the proper sampling of the target.

The operator is asked to input target characteristics, weather conditions, and other items perculiar to a particular target scene. This information is recorded on magnetic tape. The RIP is then initialized to execute the desired pattern. Any necessary angular parameters are displayed on the CRT. An initial calibration is performed at this time and the data is collected. The RIP is then commanded to scan one line of the target. From the pattern points, radiometric data from the PSD outputs are gathered and stored. If necessary, depending on a user entered option, a calibration of the radiometer is performed and the data is collected. The radiometric and calibration data from the scan is then formatted, packed, and recorded on magnetic tape.

The quick-look analysis software checks to verify proper operation of the radiometer. First, the tape is read, the header information is printed on the console, and the black and white video image is displayed on the monitor. Following this, the initial calibration information is read, converted to both volts and temperature, and displayed on the console. Finally, using the calibration information, the radiometric data is analyzed, mapped onto a pseudo color scale, and displayed on the color monitor.

3.0 Ice/Frost Signature Data Measurements

3.1 Phase 1a Program (Georgia Tech Tests)

The target used for the ice/frost data collected at Georgia Tech consisted of an ET SOFI sample attached to an aluminum substrate and conditioned to simulate ET cryogenic temperatures. For ease of operation the substrate was conditioned with LN_2 and the SOFI thickness was varied to enable ice/frost accumulations in the test enclosure. The foam-covered aluminum test panel was attached to an aluminum subpanel which was cooled with LN_2. The target was originally constructed with a transparent front, made of plexiglass, to allow viewing of the target panel from outside. During the day, however, incident sunlight trapped by the plexiglass cover kept the test panel too warm for ice to form. The plexiglass was replaced with one inch-thick styrofoam insulation with good success.

Four surface conditions for the target sample were considered for these measurements. They were dry, wet, frost and ice. A dry target was one where no moisture, frost or ice was present on the target or insulating enclosure. A dry condition was obtained at the beginning of each measurement period by opening the enclosure to the high ambient temperature and to strong incident sunlight. Water was sprayed onto the dry target to form a wet target. A uniform layer of water was applied and a wet target was obtained by closing the insulating doors to prevent rapid evaporation.

Frost and ice formation presented a more difficult task. LN_2 was pumped into a reservoir which included the aluminum sub-panel as a wall. The gaseous nitrogen was bled off by a vent from the interior of the test enclosure. The low temperature of the nitrogen exhaust cooled the surface of the foam sufficiently to allow frost to form. When the reservoir had been filled with LN_2, the target surface was placed horizontal with the SOFI facing upward. Water was poured onto the SOFI and the insulating doors were closed. The chamber was then subject to extremely rapid cooling of the air by pumping LN_2 directly into the chamber. The extremely cold ambient air froze the water directly onto

the foam, forming a nearly-uniform layer of ice. The target was then positioned to the correct angle for measurements. Ice, once formed, was maintained by the cooling effect of the LN_2 bleed off routed into the chamber. This process was repeated as often as necessary to obtain a specified thickness of ice.

The beamwidth, θ_B, of the Georgia Tech 95 GHz instrumentation radiometer is approximately 0.4 degrees. The beam spot diameter, d, on the target is given by:

$$d = R\theta_B\ (\pi/180) = 0.4R\ (\pi/180) = 6.98 \times 10^{-3}\ R$$

where R is the distance between the radiometer's lens and the target. R varying from 50 to 200 feet yielded beam spot diameters from 4.2 to 16.8 inches. The radiometer output was sampled four times per beamwidth, or once every 0.1 degree. The target size was 3 feet by 3 feet and measurements were made with the target rotated along a horizontal axis for various target deflection angles. Below is a summary of the beam spot diameter (d), the number of beams per target width, and the number of samples per scan line on the target for R = 50 feet and 200 feet.

R, feet	d, inches	Beamwidths/Target Width	# Samples/Azimuth Scan
50	4.2	8.6	34.4
200	16.8	2.1	8.6

During the course of the Georgia Tech measurements program, many scans of the target were made in order to depict a variety of target and environmental conditions. Table 4 is a summary of the data collected during the ice measurements at Georgia Tech. The target view angle is that angle between the line of sight from the radiometer to the target and the normal line from the target surface. The sky temperatures shown are the radiometric temperatures of the sky recorded at the beginning (1), the middle (2), and the end (3) of the scan. The coldest pixel temperatures refer to the lowest pixel temperature in the scan for the reference plate and for the target plate. The reference plate (aluminum sheet) was scanned concurrently with the sample target to compensate for

Table 4

Summary of Scan Data

Test	Target View Angle	Sky Temperatures 1	2	3	Coldest Pixel Temperatures Reference	Target	Ref. Avg. $\overline{R}$	Targ. Avg. $\overline{T}$	Differences T-R	$\overline{T}-\overline{R}$	Polarization	Ice Thickness	Cloud Cover Estimate	Comments
1	30°	130	128	122	167	196	179	211	29	32	Vertical	1/8"	50%	1/4" SOFI, doors, 200 feet Run # 20, Channel # Ø
2	30°	128	125	121	161	205	172	212	44	40	Horizontal	1/8"	50%	1/4" SOFI, doors, 200 feet Run # 20, Channel # 3
3	30°	73	77	78	120	125	132	136	5	4	Vertical	Dry	10%	1/4" SOFI, doors, 200 feet Run # 35, Channel # Ø
4	30°	72	72	74	89	102	108	108	13	0	Horizontal	Dry	10%	1/4" SOFI, doors, 200 feet Run # 35, Channel # 3
5	60°	145	153	145	205	228	213	238	23	25	Vertical	1/8"	90%	1/4" SOFI, doors, 200 feet Run # 21, Channel # Ø
6	60°	145	151	143	206	230	211	240	24	29	Horizontal	1/8"	90%	1/4" SOFI, doors, 200 feet Run # 21, Channel # 3
7	60°	76	75	78	183	196	206	220	13	14	Vertical	Dry	10%	1/4" SOFI, doors, 200 feet Run # 36, Channel # Ø
8	60°	72	74	76	177	192	196	206	15	10	Horizontal	Dry	10%	1/4' SOFI, doors, 200 feet Run # 36, Channel # 3
9	45°	157	130	130	159	163	170	173	4	3	Vertical	Dry	60%	1/4" SOFI, 200 feet Run # 14, Channel # Ø
10	45°	152	126	128	159	166	177	180	7	3	Horizontal	Dry	60%	1/4" SOFI, 200 feet Run # 14, Channel # 3
11	45°	128	127	130	146	195	165	210	46	45	Vertical	1/8"	40%	1/4 ' SOFI, doors, 200 feet Run # 19, Channel Ø
12	45°	126	127	128	150	201	162	211	51	49	Horizontal	1/8"	40%	1/4 ' SOFI, doors, 200 feet Run # 19, Channel # 3
13	45°	92	96	92	126	140	149	156	14	7	Vertical	Dry	5%	1/4 ' SOFI, Doors, 200 feet Run # 30, Channel # Ø
14	45°	90	95	89	114	130	134	149	16	15	Horizontal	Dry	5%	1/4" SOFI, Doors, 200 feet Run # 30, Channel # 3
15	45°	100	106	102	119	151	143	161	32	18	Vertical	1/16"	50%	1/4" SOFI, Doors, 200 feet Run # 33, Channel Ø
16	45°	97	103	99	130	155	146	168	25	22	Horizontal	1/16"	50%	1/4" SOFI, Doors, 200 feet Run # 33, Channel # 3

Note: All temperatures are in degrees Kelvin.

sky temperature variations during the scans. The averages of nine pixels in a 3 x 3 pixel square at the centers of the radiometric image of the reference ($\overline{R}$) and the target ($\overline{T}$) are computed and listed. The differences are computed between the coldest temperatures for the target and the reference shown as (T-R) and for their averages shown as ($\overline{T} - \overline{R}$). The thickness of the ice, or its absence, is listed, followed by the percentage of cloud cover observed during the scan. Under comments, the thickness of the Spray-On-Foam Insulation (SOFI) on the target is listed; "doors" indicate the presence of one inch thick styrofoam doors over the target; and the run and channel numbers are given as a source to refer back to the original data for future analysis.

3.2 Phase 1b Program (NSTL Tests - Dec. 1980 & Jan. 1981)

Based on the Georgia Tech ice measurements using the ET target samples, the next measurements called for ice/frost detection on the shuttle external tank during actual cryogenic loading operations. The site for these measurements was at NASA's National Space Test Laboratory (NSTL) near Bay St. Louis, MS where the orbiter engine static firing tests were held. Reference targets located on the test stand were scanned concurrently with the ET in order to compensate for the variation in the background sky. One reference target was an aluminum sheet of 1/16 inch thickness with approximate dimensions of 4 feet by 8 feet. The second reference target was an aluminum sheet covered with SOFI and located adjacent to the metal target. Both reference targets were tilted about 15° upward toward the sky in order to provide an acceptable angle of sky reflection. Figure 11 is a photograph showing both targets on the test stand.

The 95 GHz radiometer used for NSTL measurements has a 20 inch diameter (D) lens resulting in a 0.4° half power beamwidth (θ_B°) at 95 GHz. The beam spot diameter, d, on the ET surface at a distance R from the radiometer was previously shown to be:

$$d = R\,\theta_B^\circ \left(\frac{\pi}{180}\right).$$

Table 5 summarizes the spatial resolution for the 95 GHz radiometer used for the measurements at NSTL. At a distance of 450 feet the beam spot diameter was 3.14 feet. This resulted in approximately nine beamspots across the 28 foot diameter ET target at a distance of 450 feet. Table 5 also shows the number of beam spots per scan across the external tank as a function of range R.

The measurement program at NSTL required additional support for the Georgia Tech radiometer and operating personnel. The basic facility support included the following:

1) A forklift was required to maneuver the radiometer instrument onto the antenna positioner;
2) A supply of liquid nitrogen of about 160 liters per day was used for the radiometer's cooled calibration loads,

Figure 11. Radiometric Reference Targets Used at NSTL During 95 GHz Ice Measurements.

Table 5

95 GHz Radiometer Spatial Resolution Data For
ET Scan at NSTL

R (feet)	d (feet)	Beam spots/scan cross ET
200	1.40	20.0
250	1.75	16.0
300	2.09	13.4
350	2.44	11.5
400	2.79	10.0
450*	3.14	8.9
500	3.49	8.0

*Approximate distance between ET and Georgia Tech radiometer site for all tests at NSTL.

3) A 4 by 8 foot aluminum plate of 1/16 inch thickness was provided to serve as the secondary reference target and was mounted near the ET LOX tank on the tower;

4) Electrical power requirements for the radiometer system of 110 Vac, 60 Hz, 50 amperes maximum were provided during the NSTL tests.

During the January 1981 NSTL tests Georgia Tech requested that NASA provide a cut-out section of 1 meter square on the LOX tank. This was requested to allow a better opportunity for ice to form on the ET where the SOFI thickness was reduced. The thickness of the SOFI was reduced to 1/2 inch in the cut-out area. Figure 12 is a close-up view of this area. Following the loading of the ET with liquid oxygen and liquid hydrogen, Georgia Tech personnel sprayed the cut-out area with freon and water to form ice. This region was scanned continuously with the remaining ET target where no ice was seen. The total scan sequence included 1 hour of data prior to ET loading, 5.5 hours of data taken with the tank partially or fully loaded, and 1.5 hours of data collected immediately after engine firing.

Figure 12. Close-up View of 1 Meter Square Cut-out Section Located on ET LOX Tank.

Table 6

Summary of Effects of Ice

View Angle	Polarization	Ice Thickness	Temperature Change Due to Ice: Coldest Pixel $(T-R)_{ICE} - (T-R)_{DRY}$	Temperature Change Due to Ice: Center Average $(\overline{T}-\overline{R})_{ICE} - (\overline{T}-\overline{R})_{DRY}$	Test Compared (See Table 4): Ice	Test Compared (See Table 4): Dry
30°	Vertical	1/8"	24	28	1	3
30°	Horizontal	1/8"	31	40	2	4
60°	Vertical	1/8"	10	11	5	7
60°	Horizontal	1/8"	9	19	6	8
45°	Vertical	1/8"	42	42	11	9
45°	Horizontal	1/8"	42	46	12	10
45°	Vertical	1/16"	18	11	15	13
45°	Horizontal	1/16"	9	7	16	14

Note: All temperatures are in degrees Kelvin.

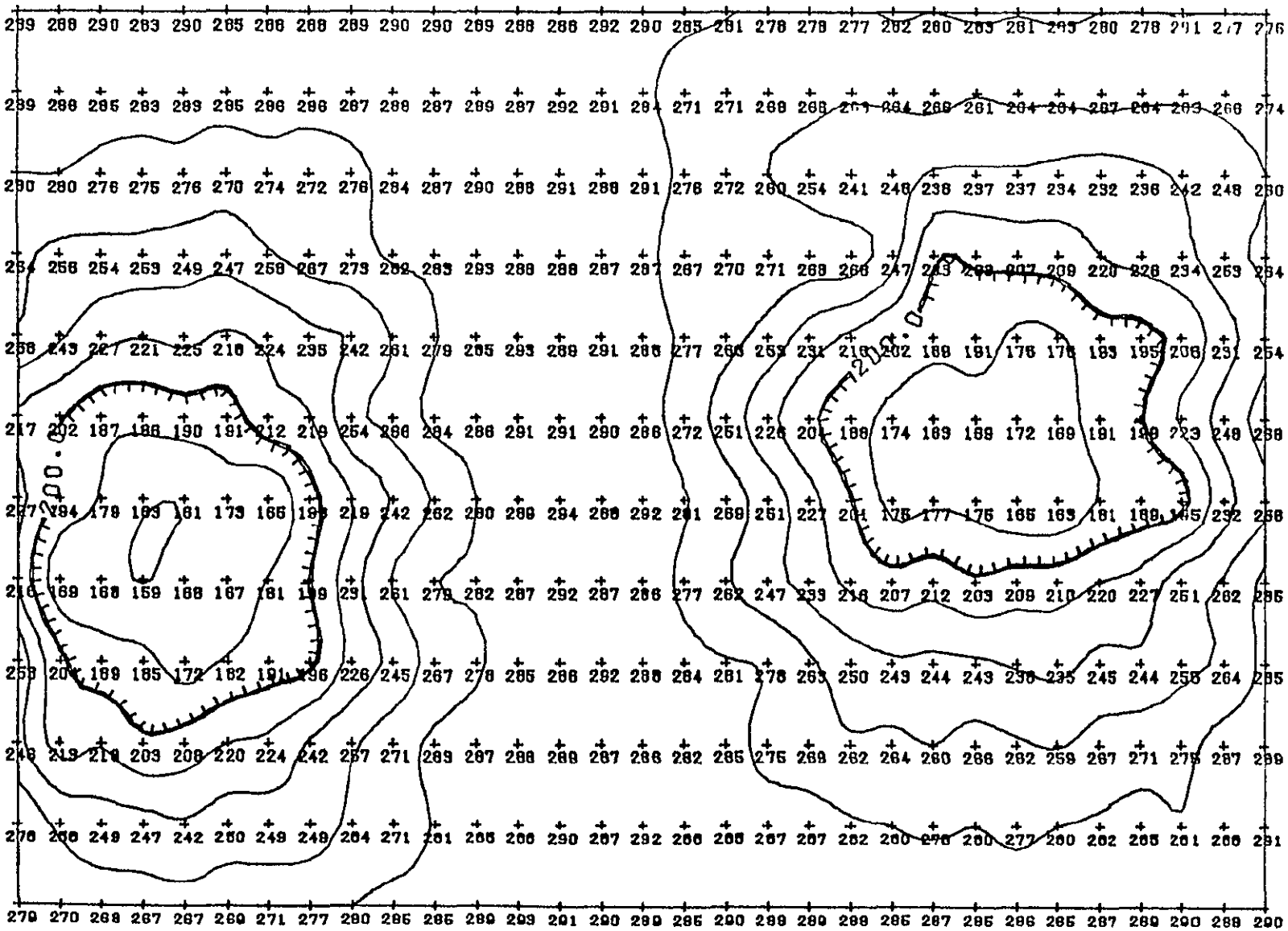

Figure 13. 95 GHz Pixel Temperature Contour Plot for Run #14, Channel #0 with Reference Target on Left and ET Target (Dry) on Right.

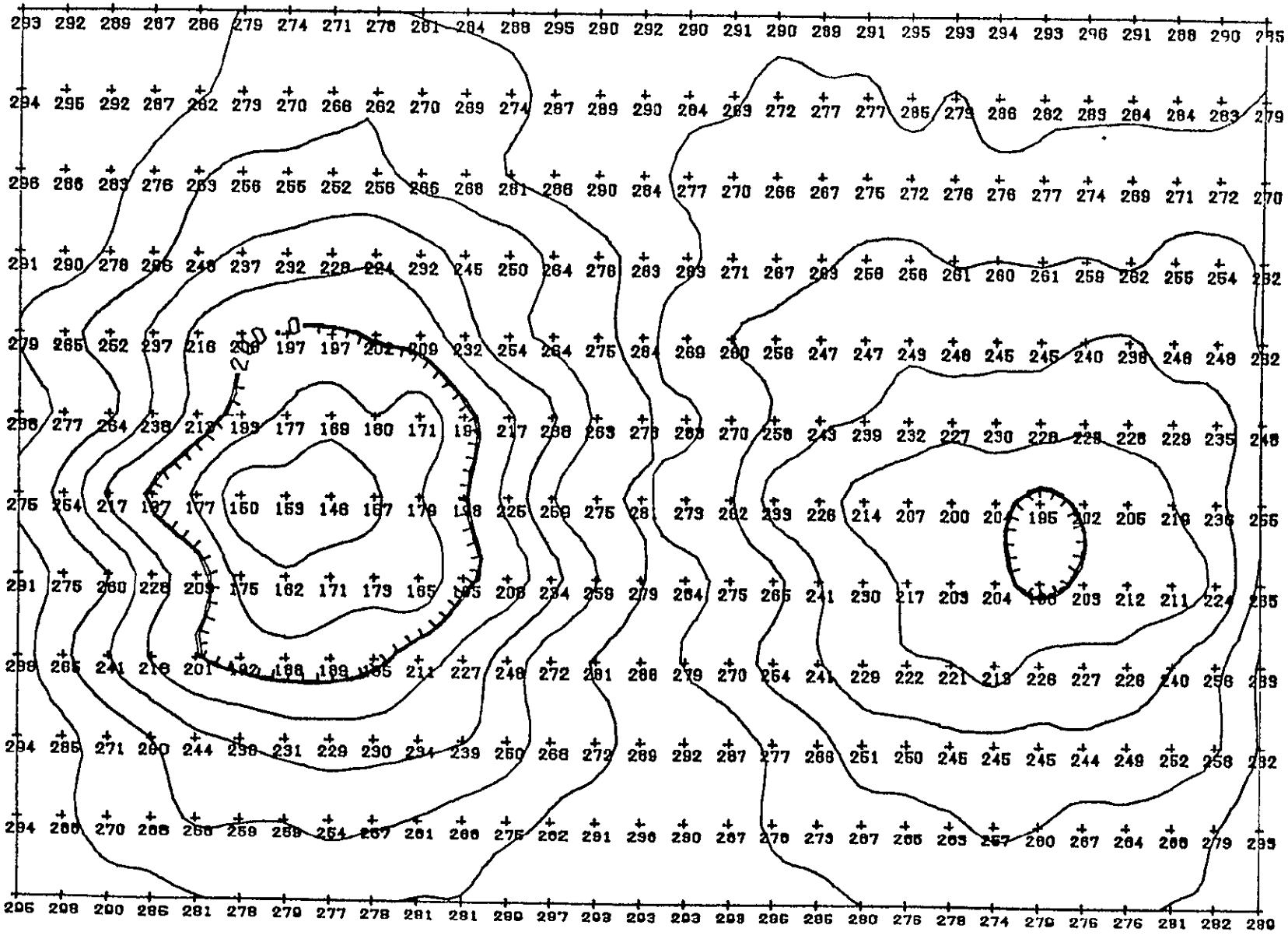

Figure 14. 95 GHz Pixel Temperature Contour Plot for Run #19, Channel #0 with Reference Target on Left and ET Target (with Ice) on Right.

45°K indicating that the ET target's apparent temperature rose approximately 42°K when covered with ice.

Figure 15 is a radiometric scanned image at 95 GHz of the scene showing the reference target on the left and the dry ET target sample on the right. This image is of the same data run #14, Channel #0 described above. The color breakpoints for the image were set with dark blue as the coldest temperature displayed and light blue as the warmest temperature. Figure 16 is the radiometric image of the target following ice formation of approximately 1/8 inch thickness on the target sample. The ET target appears warmer (pinkish color) due to the presence of ice.

Another technique used to compare the sets of data (with and without ice) was the generation at Georgia Tech of three dimensional plots of the data array. Again a comparison is made between run #14 (dry target) and run #19 (ice layered target) using the pictorial information as shown in Figures 17 and 18. For these plots the reference target is shown on the left and the ET sample is on the right. The decrease in the height of the ET sample plot is indicative of an increase in the radiometric temperature due to ice being present.

4.2 Phase 1b Data (NSTL Tests - Dec. 1980 & Jan. 1981)

The data gathered during the NSTL tests provided a good data base for the signature analysis because of the availability of an actual external tank fully loaded with cryogenics. The location of the radiometer, within 450 feet of the ET, provided good spatial resolution needed for the generation of radiometric images of the target. The control test of forming ice on the cut-out section (with reduced SOFI thickness) offered a comparison of ice data and dry target data using processing techniques developed at Georgia Tech.

Figure 19 is a collection of 95 GHz radiometric images (16) of the ET LOX section in which eight hours of continuous scans were performed beginning with pre-loading of cryogenics and ending with post-firing of the orbiter engines. Each of the 16 images shown represent a 30 minute scan of the ET and includes the cut-out area with SOFI thickness reduced to approximately 1/2-inch. Table 7 provides a legend for each

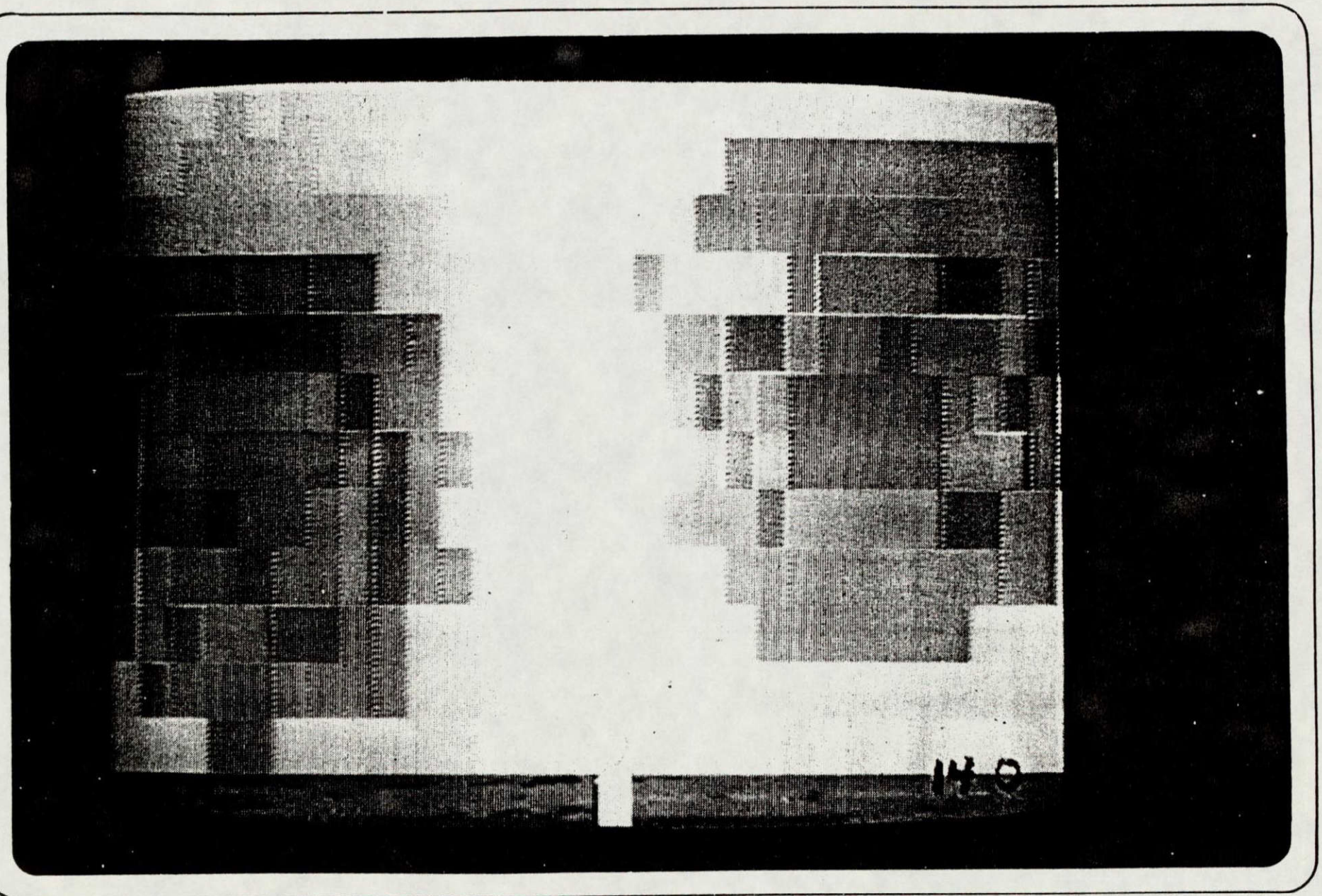

Figure 15. 95 GHz Radiometric Image for Run #14, Channel #0 with Reference Target on Left and ET Target (Dry) on Right.

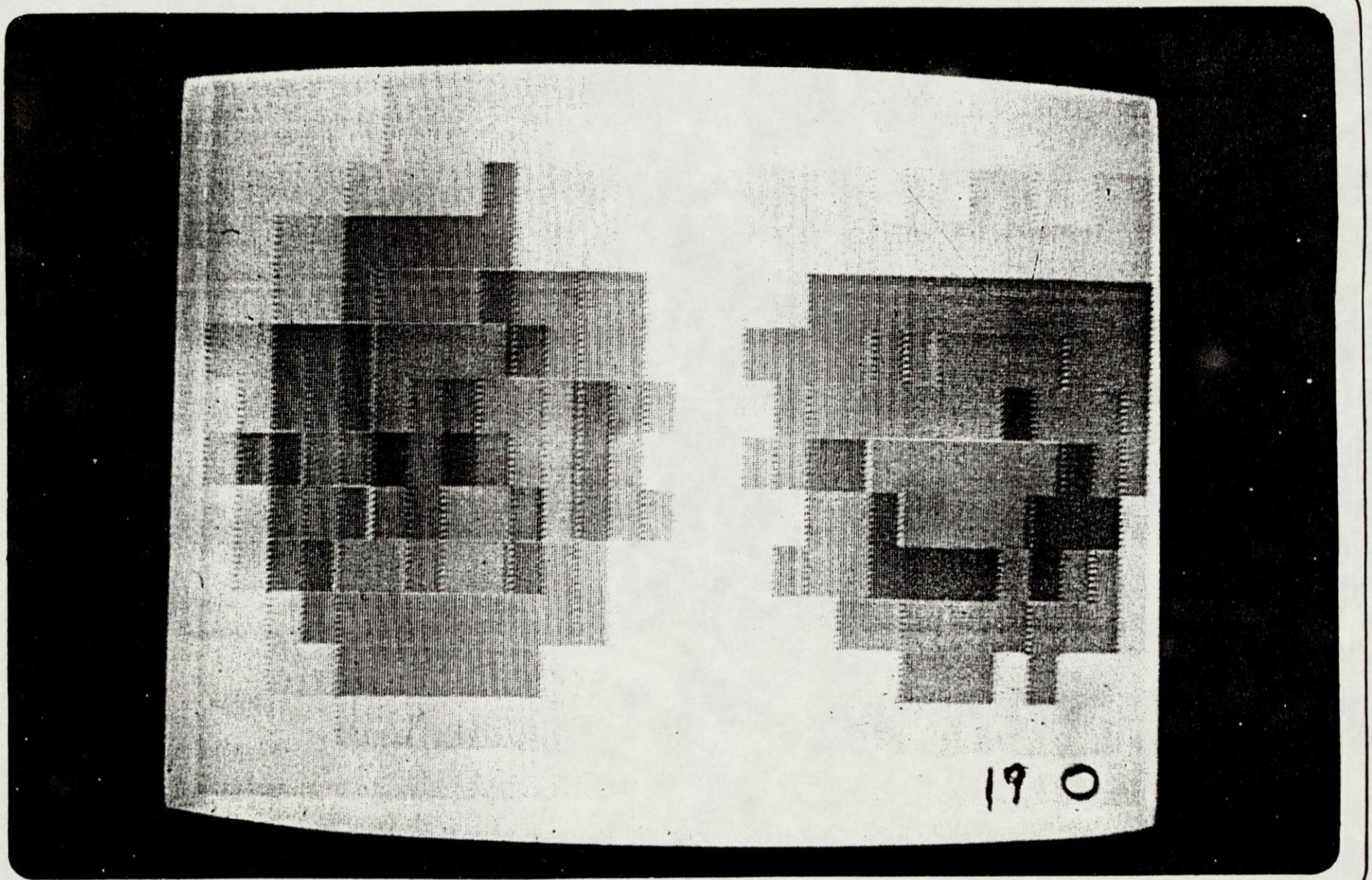

Figure 16. 95 GHz Radiometric Image for Run #19, Channel #0 with Reference Target on Left and ET Target (with Ice) on Right.

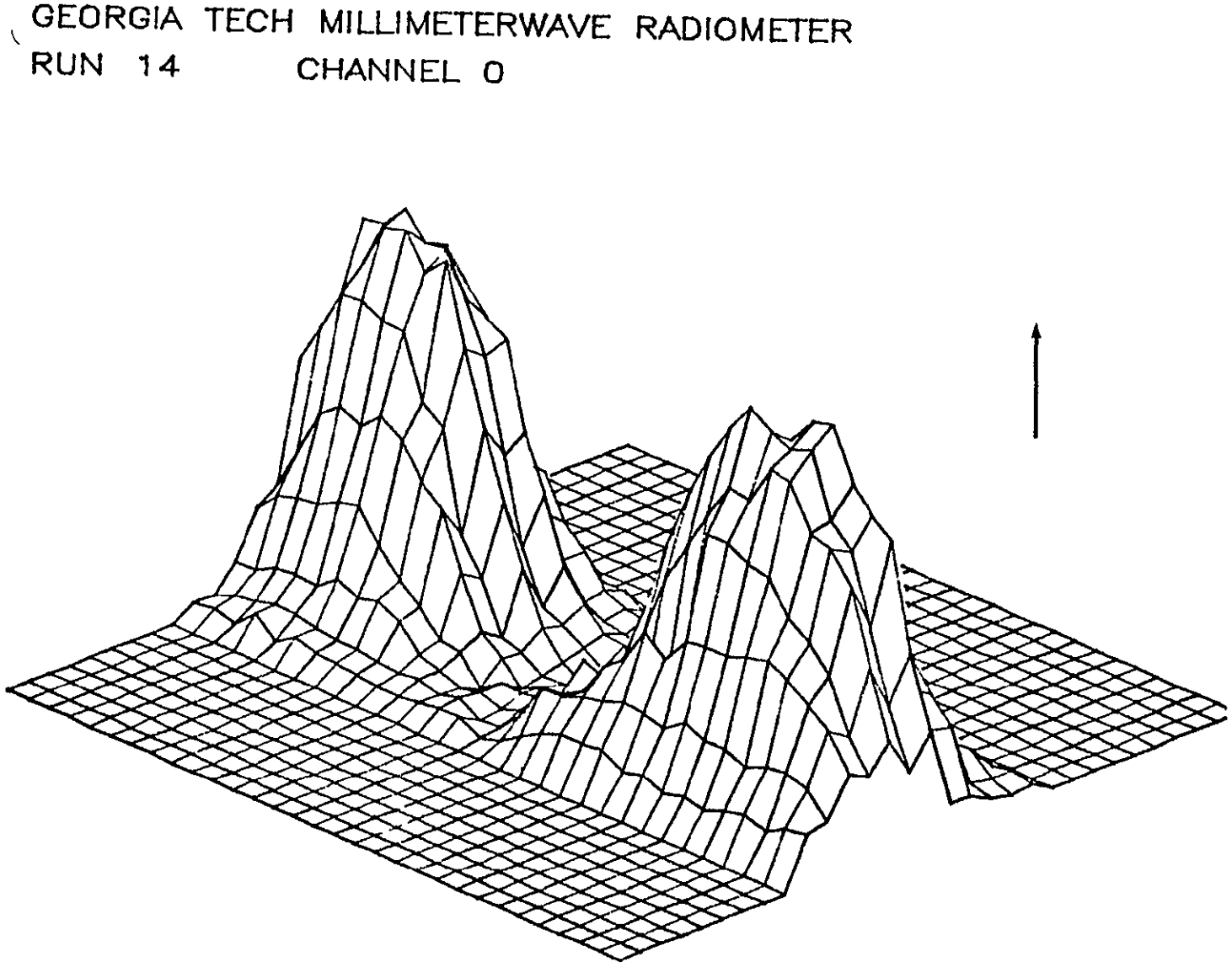

Figure 17. 95 GHz 3D Plot with Reference Target on Left and Dry ET Target on Right.

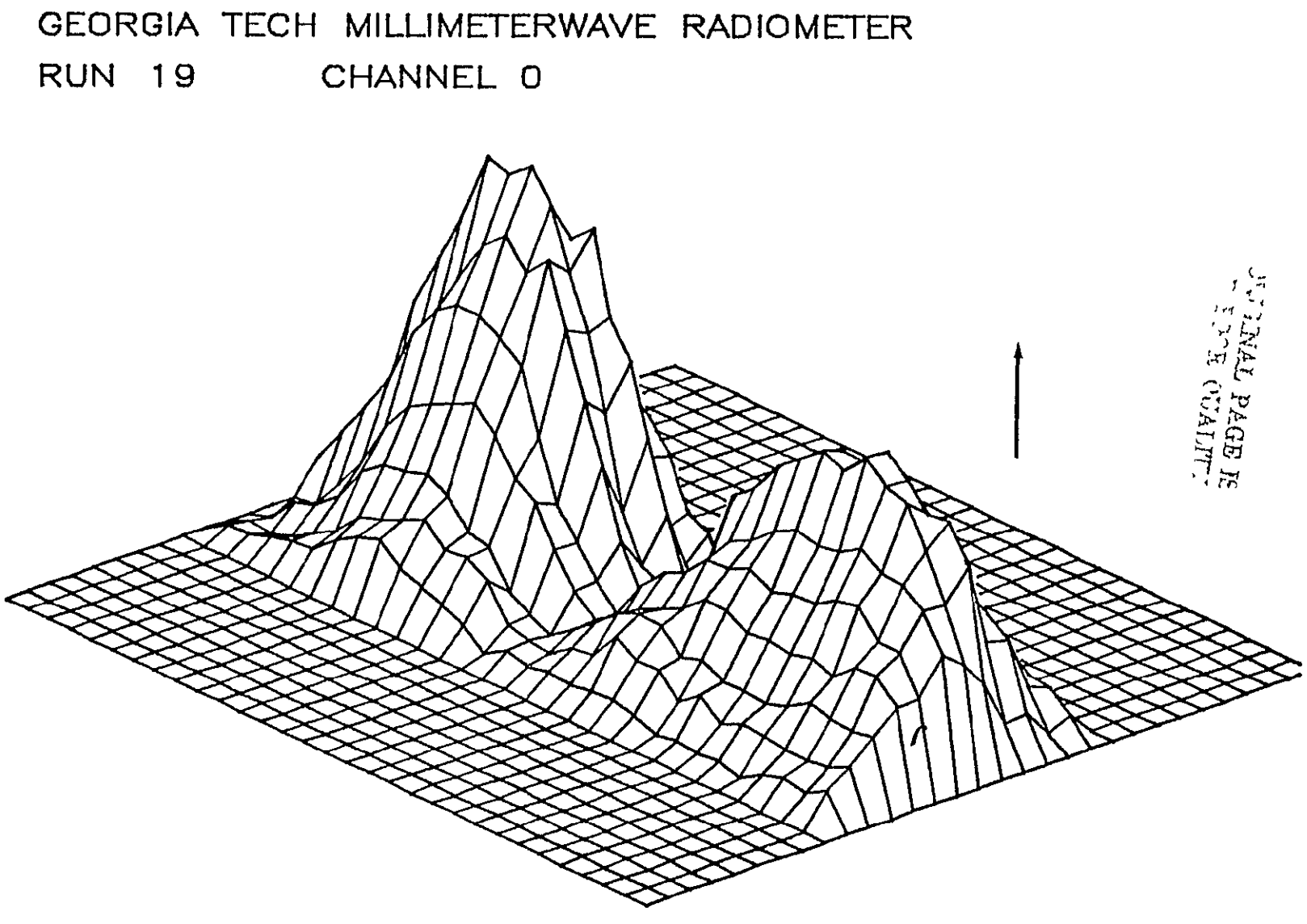

Figure 18. 95 GHz 3D Plot with Reference Target on Left and Ice Covered ET Target on Right.

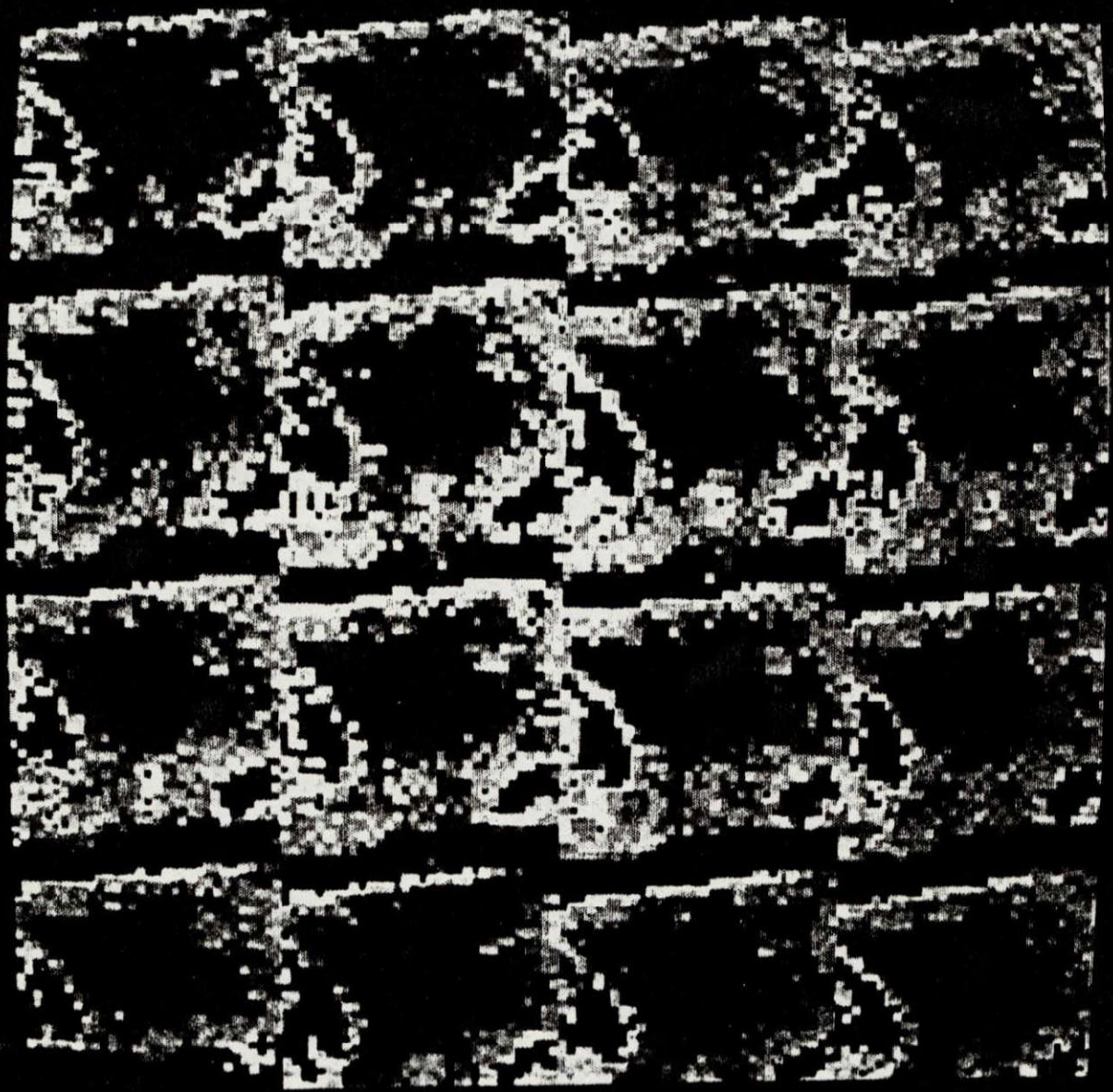

Figure 19. 95 GHz Imaging Scan Sequence of Shuttle ET at NSTL.

individual scan from pre-load to post-fire. During scan 10, ice was artificially formed on the cut-out area after the ET was fully loaded with cryogenics. Observe in Figure 19 that the cut-out area image shows a more reddish color which represents an increase in radiometric temperature. Detailed analysis revealed an increase of about 20°K due to ice formation on the ET which indicated a reduction in the cold sky reflection off the surface of the cut-out area.

Data analysis routines for the mean, standard deviation, and the variance of the NSTL ice signature data were developed during this program. Emphasis was placed on that data gathered during the January 1981 NSTL tests where ice signatures were collected from the cut-out area on the ET. Figure 20 is the view of the ET LOX section with selected portions of the ET target as shown. Locations of interest within the radiometer's scan pattern are further described in Table 8. Section 11 is the cut-out area with reduced foam thickness. The cut-out area is contained within the larger area designated as 9. Table 9 illustrates an example of the ice signature statistical data available. Data run #149 was the last 30 minute scan performed prior to the artificial formation of ice on the ET cut-out region. Data run #150 was the following scan which included the presence of ice. An increase in radiometric mean temperature of approximately 20K from run #149 to #150 on the sections 9 and 11 is evident from Table 9. Visual inspection during the NSTL tests revealed that ice was present on the cut-out section resulting in an apparent warming in the radiometric temperature.

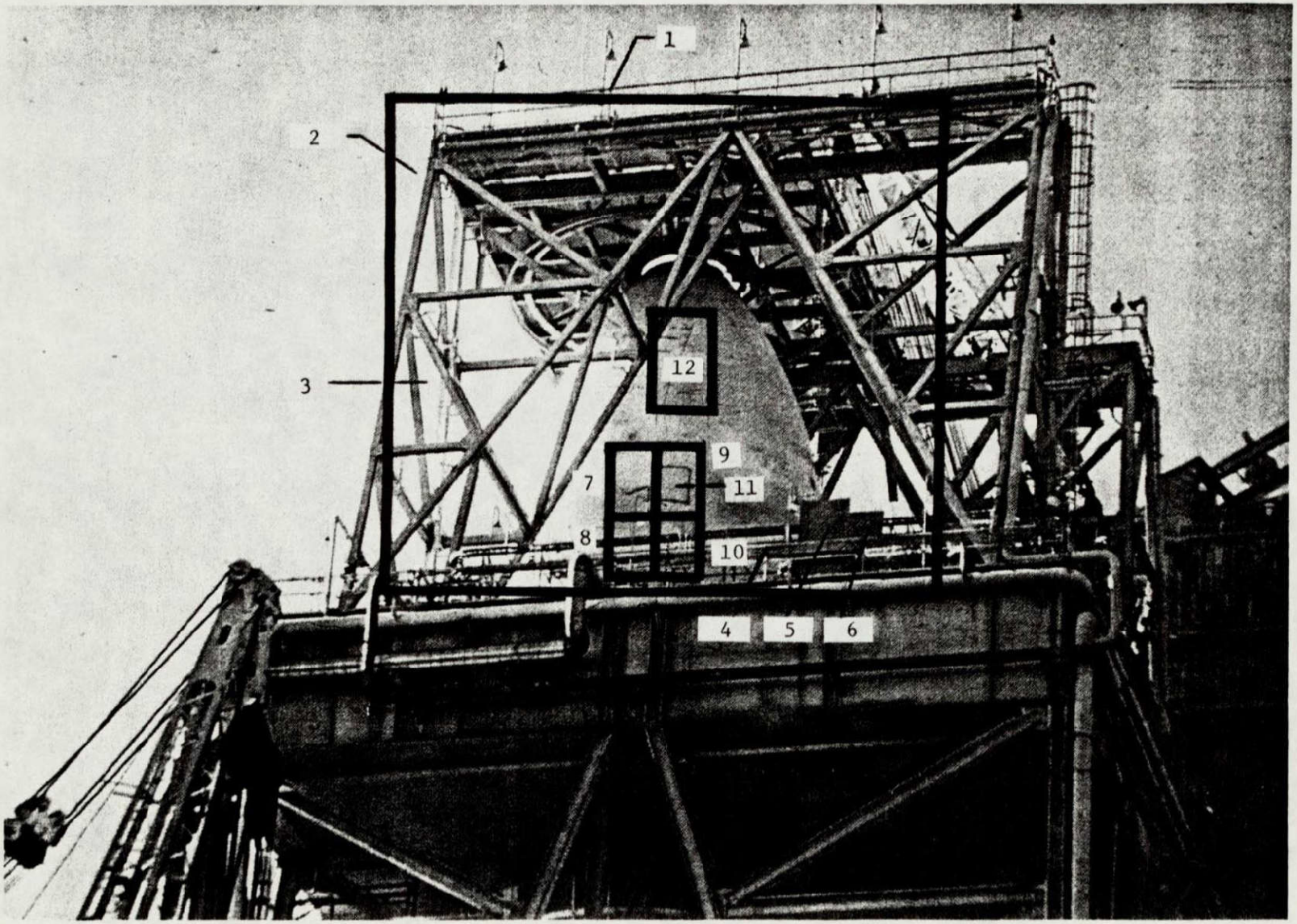

Figure 20. View of ET LOX Section at NSTL as Seen by 35/95 GHz Scanning Radiometer. (Refer to Table 8 for section call out.)

ORIGINAL PAGE IS
OF POOR QUALITY

Table 9

NSTL Data Runs (Scans) #149 and #150 from 95 GHz
Vertical Polarization Radiometric Data Output

SECTION	TL COORDS		LR COORDS		NPTS	MEAN	VARIANCE	STD DEV
1	0,	0	32,	31	1056	145.2	839.3	28.97
2	0,	0	5,	2	18	74.3	321.1	17.92
3	1,	18	4,	21	16	104.9	221.1	14.87
4	21,	29	33,	32	52	187.5	260.8	16.15
5	25,	22	27,	26	15	98.2	251.2	15.85
6	28,	23	29,	26	8	104.4	464.3	21.55
7	12,	20	14,	24	15	149.0	37.5	6.13
8	12,	25	14,	29	15	152.1	128.9	11.35
9	15,	20	17,	24	15	130.4	155.7	12.48
10	15,	25	17,	29	15	146.0	388.3	19.70
11	15,	22	17,	23	6	124.1	123.8	11.13
12	15,	10	18,	15	24	186.3	26.0	5.10

a) RUN 149 CHANNEL 0
TH= 333.10 TC= 80.51 TSKY= 29.21 TLEN= 276.25
SCENE SIZE IS 33 PIXELS BY 33 ROWS
MIN AND MAX TEMPS ARE : 47, 212

SECTION	TL COORDS		LR COORDS		NPTS	MEAN	VARIANCE	STD DEV
1	0,	0	32,	31	1056	147.6	811.0	28.48
2	0,	0	5,	2	18	71.7	150.2	12.25
3	1,	18	4,	21	16	108.0	216.1	14.70
4	21,	29	33,	32	52	187.5	184.1	13.57
5	25,	22	27,	26	15	101.2	354.1	18.82
6	28,	23	29,	26	8	111.2	173.0	13.15
7	12,	20	14,	24	15	148.8	79.1	8.89
8	12,	25	14,	29	15	156.6	87.5	9.36
9	15,	20	17,	24	15	148.3	36.0	6.00
10	15,	25	17,	29	15	154.4	98.2	9.91
11	15,	22	17,	23	6	144.0	8.3	2.88
12	15,	10	18,	15	24	186.0	42.6	6.53

b) RUN 150 CHANNEL 0
TH= 333.12 TC= 80.51 TSKY= 29.63 TLEN= 277.49
SCENE SIZE IS 33 PIXELS BY 33 ROWS
MIN AND MAX TEMPS ARE : 42, 205

TH = hot calibrate load (^{o}K)
TC = cold calibrate load (^{o}K)
TSKY = sky temperature (^{o}K)
TLEN = antenna lens (^{o}K)
MIN and MAX Temps = minimum and maximum temp. (^{o}K) for run
TL COORDS, LR COORDS = top-left and lower right coordinates for each section
NPTS = number of sample points in section
MEAN = section mean temp. (^{o}K)
VARIANCE, STD DEV = variance and standard deviation (^{o}K) for section

5.0 Conclusion

The tests at Georgia Tech and at NSTL as well as the follow-up data analysis programs have proven the usefulness of millimeter wave radiometry techniques for the detection of ice formation on the shuttle external tank. The measurements revealed that ice on the ET resulted in an increase in the radiometric temperature of the ET surface due to reduced sky reflection from the target. Following these tests Georgia Tech modified the instrumentation radiometer by replacing the 20 inch lens with a 4 foot dish antenna. Figure 21 is a photograph of the modified radiometer. This change was performed to provide a smaller beam spot size for improved spatial resolution. Table 10 provides information on the instrument's capabilities for target detection for range $R \geq 450$ feet. The target range shown is consistent with information from NASA on sensor to ET target distances anticipated at the space shuttle launch facility.

The data analysis programs generated by Georgia Tech demonstrated that on-line processing of ice signatures collected during shuttle pre-launch operations could be used to aid NASA in determining a go or no-go launch. Follow-up measurements with improved spatial resolution would offer additional evidence of the usefulness of millimeter wave radiometry to support the ice detection measurements for the shuttle launch program.

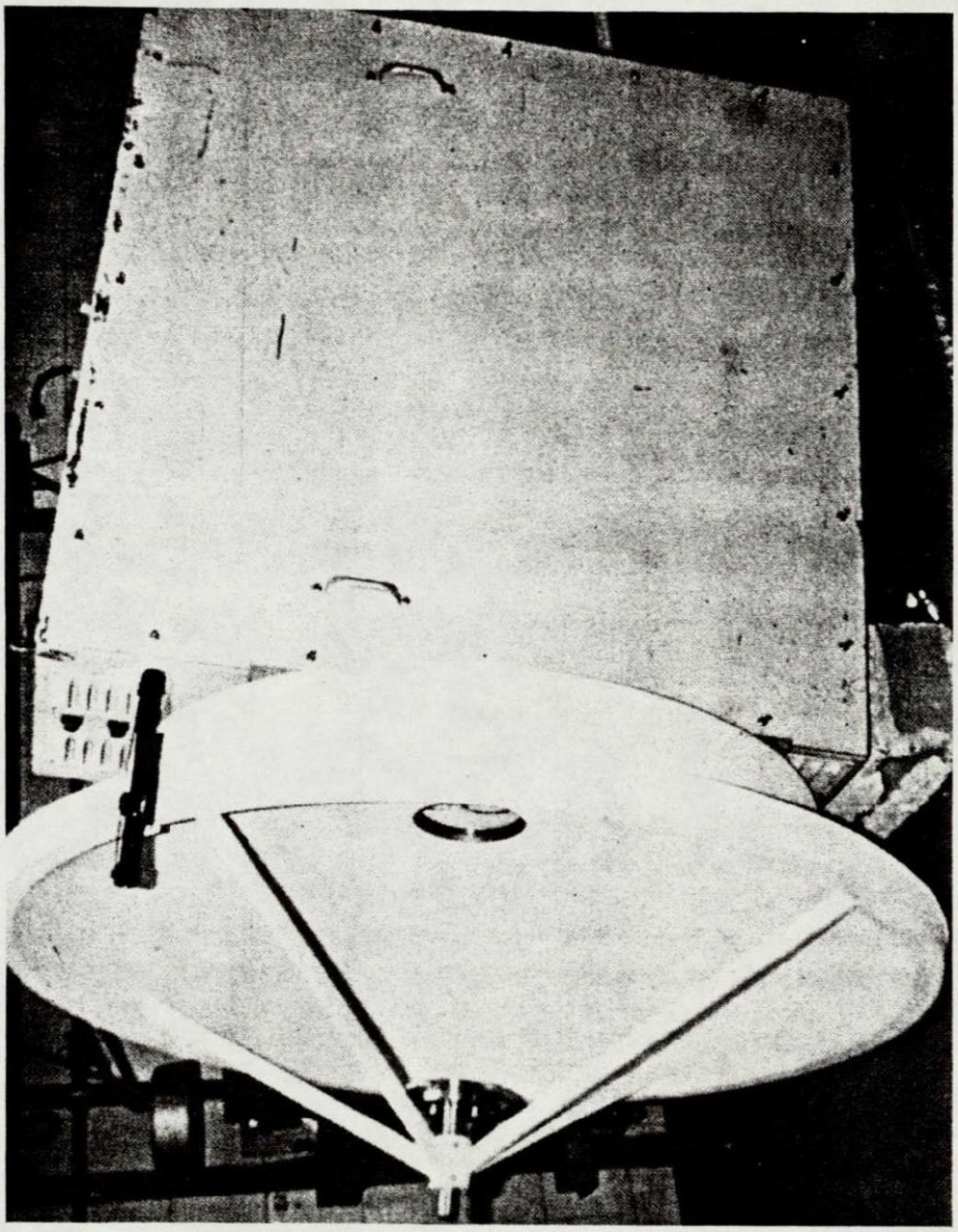

Figure 21. Georgia Tech 35/95 GHz Instrumentation Radiometer with 4-Foot Dish Antenna.

Table 10

95 GHz Radiometer Spatial Resolution Data Using 4-Foot Antenna Dish (Note 1)

R(ft)	d(ft)	$A_T(ft^2)$
450	1.728	2.345
500	1.920	2.895
550	2.112	3.503
600	2.304	4.169

Note 1. $d = R\theta^\circ(\frac{\pi}{180})$, for $\theta^\circ = 0.22$ degrees and $A_T = \frac{\pi d^2}{4}$.